

Selective Rydberg-level population of multiply charged ions at solid surfaces: A dynamic theory for low-angular-momentum ionic states

N. N. Nedeljković and Lj. D. Nedeljković

Faculty of Physics, University of Belgrade, P.O. Box 550, 11001 Belgrade, Yugoslavia

S. B. Vojvodić

Institute of Biophysics, Faculty of Medicine, Višegradska 26/2, 11001 Belgrade, Yugoslavia

M. A. Mirković

Faculty of Physics, University of Belgrade, P.O. Box 550, 11001 Belgrade, Yugoslavia

(Received 18 February 1993; revised manuscript received 12 November 1993)

Selective Rydberg-level population of multiply charged ions (e.g., $Z=6, 7,$ and 8) at solid surfaces is treated in normal emergence geometry. For the intermediate ionic velocity region (between $v \approx 1$ and 3 a.u.) a molecular-dynamics-type model of the electron pickup process from the solid valence band into low-angular-momentum ionic states ($l=0, 1,$ and 2) is proposed. Specific features of the Rydberg states and ions (large size, high degeneracy with respect to l , high value of Z) are included in the model. The electron transition amplitude is calculated as a mixed electron-density flux through a moving Firsov plane, whose kinematics is determined by a variational requirement. A multichannel character of the process is taken into account in the framework of a statistical treatment of decoupled channels, based on the approximation of small transition probabilities. The population probability $P_{nl} = P_{nl}(v, Z)$ of the (n, l) state is in sufficiently good agreement with available beam-foil experimental data (S VI, Cl VII, Ar VIII) not only as a function of the principal quantum number n , but also as a function of l and v . An "anomalous" peak at $n=11$ in the population probability of Ar VIII is briefly discussed from the standpoint of the developed formalism. The predicted maxima in the v dependence of $P_{nl}(v, Z)$ in the intermediate velocity region calls for further more refined experimental studies.

I. INTRODUCTION

The Rydberg-level population of multiply charged ions in the presence of a solid surface has been studied in many beam-foil experiments. In this paper we discuss the case of multiply charged ions (e.g., $Z=6, 7,$ and 8) moving with intermediate velocities ($v = \text{few a.u.}$).¹⁻⁸ This region of ionic parameters Z and v is characterized by a selective population of Rydberg levels with principal quantum number $n \approx Z$. Although some relevant conclusions about this effect have been known for a relatively long time,⁷ its basic quantum mechanisms are not yet well understood.

The selective Rydberg-level population was established under rather limited experimental conditions. Carbon foils have mainly been used and only a few kinds of ionic projectiles (e.g., the hydrogenlike ions S VI, Cl VII, and Ar VIII, but also the heliumlike species of Kr VIII and Xe VIII) were investigated in a more or less systematic way. In all cited experiments the normal emergence geometry has been used, whereas the relevant relative level population probabilities were measured exclusively by methods of optical spectroscopy. Most frequently, the population probability as a function of the principal and angular momentum quantum numbers (n and l) has been investigated; only one paper⁴ reports its velocity dependence.

It has been suggested many times (see, e.g., Refs. 1 and

7) that the levels with $n \approx Z$ are populated through electron pickup from the valence band of the foil, in the outgoing part of the ionic trajectory. This suggestion is based on both energetic and geometrical reasons. Namely, the electron binding energies of the carbon foil valence band are comparable with the binding energies of the formed ionic Rydberg states $n \approx Z$, and near-resonant character of the electron pickup is expected. On the other hand, the mean radius $\langle r_{nl} \rangle$ of the Rydberg state (n, l) is large in comparison with mean distances between foil atoms. So, it was concluded that the Rydberg states cannot exist in undisturbed eigenstates as long as the ionic projectile is inside the foil; consequently, the electron pickup can take place only at the back of the foil.

Attempts^{6,7} to calculate the population probability P_{nl} of Rydberg levels (n, l) around $n \approx Z$ were done by using a simple quasistatic quantum model⁹ (essentially developed for thermal velocities of weakly charged ions). This model is based on a two-step procedure. In the first step the transition probability per unit time is obtained for a fixed ion (i.e., by taking the ion-surface distance R to be constant). In the second step the dynamics of ionic motion is formally introduced (taking simply $R = vt \neq \text{const}$, t being time), which leads to the formula $P_{nl}(v) = 1 - \exp(-\text{const}/v)$. Comparison of the predictions of this model with experimental facts¹⁻⁸ was only partly successful.^{7,8}

This consequence could be expected because the quasi-

static model contains several important limitations, which can be avoided only in a more consistent quantum model. Let us note, first of all, that $P_{nl}(v)$, described by the cited formula, represents the monotonically decreasing function of v , which is (as we shall see) in contradiction with the available experimental data.⁴ A more consistent treatment of the electron pickup into a moving Rydberg state must be based on a dynamic quantum model. Indeed, at intermediate velocities we are actually faced with an essentially nonadiabatic phenomenon, so that the ionic motion must be included from the very beginning.

In addition, because of the supposed resonant character of the electron transition the quasistatic model represents essentially a two-state (or one-channel) theory. Namely, it is supposed that the electron capture into a given Rydberg state (n, l) is not affected by the presence of remaining open channels leading to all other ionic states. However, in the case of the population of Rydberg states such a supposition is essentially incorrect. Indeed, the distances between Rydberg levels are small and all channels participate simultaneously. Thus, a correct description of their population requires a multichannel theory.

Some specific geometrical features of Rydberg states may also be relevant for a more consistent treatment of the process under consideration. First, the large Rydberg state can be relevant not only in the discussion of the possibility of formation of such a state inside the foil but also in the analysis of its formation at the back of the foil. Second, in spite of the fact that the electron pickup is a tunneling process of a strictly quantum-mechanical nature, the formed Rydberg ion possesses some characteristics of a quasiclassical object.

So, it is reasonable to expect that the Rydberg states are formed preferentially at sufficiently large ion-surface distances R where stable quasiclassical orbits of captured electron are possible. Moreover, the heuristic quasiclassical picture suggests that the eccentricity

$$\epsilon_{nl} \sim \left[1 - \left(\frac{l+1}{n} \right)^2 \right]^{1/2}$$

of those orbits plays an important role. Namely, in the case of lower values of l (e.g., $l=0, 1, 2$) the eccentricity ϵ_{nl} will be high and we can expect that the electron density distribution of the formed Rydberg state (n, l) is mainly localized around the ionic trajectory. However, for higher values of l the values of ϵ_{nl} will be small, which indicates not only a large size, but almost spherical electron-density distribution.

Therefore, for lower l it is reasonable to assume that only the narrow cylindrical region around the direction of the projectile motion is relevant for the electron pickup process. On the other hand, for higher l we can expect a spreading of active electron "paths" away from the narrow cylindrical region. In other words, a "tube" of relevant paths of active electrons in the pickup process has different cross sections for different values of l : whereas for $l \approx 0$ the "tube" is stringlike; for $l \approx n$ we can expect a conelike structure of the electron path set.

We developed a dynamic quantum model describing formation of low-angular-momentum Rydberg states in the process of under-barrier electron transitions. Our model is of a molecular type: the ion-solid system is considered a "supermolecule" so that the formation of bound ionic states can be seen as "dissociation" of that molecularlike system, caused by ionic motion. The present model represents further elaboration of our molecular model, developed for ground hydrogen state population at solid surfaces (in the intermediate projectile velocity region).¹⁰ Namely, in this paper we shall show that the mentioned specific features of the low-angular-momentum Rydberg states can be incorporated in that model.

The electron transition amplitude is calculated as a mixed electron-density flux through the central part of the moving Firsov plane,¹⁰ located between a solid surface and projectile. Our evaluation of the transition amplitude essentially represents a generalization of the Demkov-Ostrovskii asymptotic theory¹¹ of charge exchange in ion-atom collisions at arbitrary velocities. We generalized the Demkov-Ostrovskii's model by treating the Firsov plane kinematics in a variational manner. The multichannel character of the Rydberg state population process is taken into account in the framework of a statistical treatment of decoupled channels, based on the approximation of small transition amplitudes.

As we shall see, the calculations performed in the framework of the proposed model show that the electron transitions are nonresonant. The dependence of the obtained population probability $P_{nl} = P_{nl}(v, Z)$ on n (for fixed l) is in good agreement with experimental data. Also, the l dependence of P_{nl} (for fixed n) follows the experimental findings in the region of lower l . The main advantage of the proposed dynamic model (in comparison to the quasistatic one) lies in the fact that it reveals velocity dependence of P_{nl} : it reproduces $P_{nl}(v)$ maxima just in the intermediate velocity region, which available experimental data⁴ show. Some additional predictions of the dynamic model call for further more systematical and refined experimental studies.

Atomic units ($e^2 = \hbar = m_e = 1$) will be used through the paper unless indicated otherwise.

II. FORMULATION OF THE PROBLEM

For the purpose of this paper we set the origin of the Cartesian coordinate system S at a solid surface [Fig. 1(a)]. We consider the ionic core as a structureless, pointlike charged particle. Restricting ourselves to the case of the normal emergence geometry we assume that the ion-surface distance R depends on time t according to the classical law $R = vt$. Besides the system S , a moving coordinate system S' will be used whose origin is placed at projectile.

The Hamiltonian of the active electron is defined by¹⁰

$$H = -\frac{1}{2}\nabla^2 + U_A(\vec{r}_A) + U_M(z) + U_{AM}(\vec{r}, \vec{R}), \quad (2.1)$$

where $\vec{r}_A = \vec{r} - \vec{R}$ stands for the instant position of the active electron with respect to the moving system S' . The ionic core potential U_A is defined by $U_A = -Z/r_A$ (outside the solid, $z > 0$) and by $U_A = 0$ (inside the solid,

$z < 0$). For $z < 0$ we take $U_M = -U_0$ (where U_0 denotes the depth of solid potential well in the Sommerfeld model), whereas for $z > 0$ we set the electron self-image potential $U_M = -1/4z$. For U_{AM} outside of the solid ($z > 0$) we take the interaction potential of the active electron with ionic core image,

$$U_{AM} = Z / \sqrt{x^2 + y^2 + (z + R)^2}.$$

For $z < 0$ we set $U_{AM} = 0$.

The potentials U_A , U_M , U_{AM} , and $U = U_A + U_M + U_{AM}$ along the positive part of z axis (and for sufficiently large R) are illustrated in Fig. 1(b). Also, in the same figure we marked the instant position of the Firsov plane S_F . Note that on the right side of the S_F plane we can roughly take $U \approx U_A$, i.e., the Coulomb potential U_A is dominant. However, on the left side of the S_F plane all terms in U participate significantly. Difficulties with forms of U_M and U_{AM} in the near surface region, fortunately, are not essential¹⁰ for the calculation of asymptotic population probabilities (for large R). The

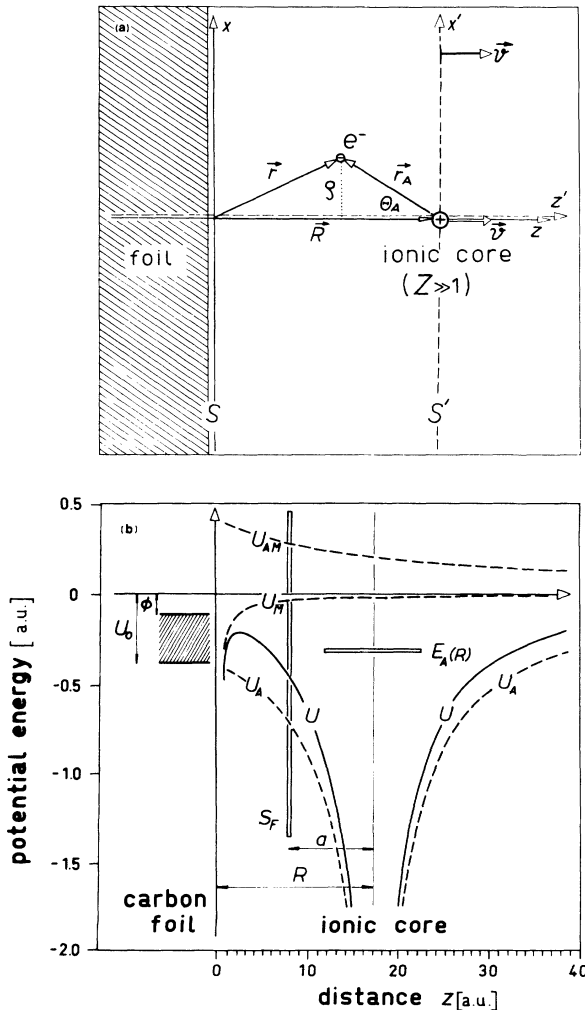


FIG. 1. (a) Geometry of the process. (b) Energies of the process in the stage when the electron capture probability reaches maximum.

same holds for nonlinear polarization effects¹² caused by a high value of the ionic charge Z .

The electron pickup process is considered¹⁰ as an electron transition from a solid eigenstate Φ_M^γ (at time $t=0$) to a moving atomic state φ_A^{nl} (at $t \rightarrow \infty$). The initial state Φ_M^γ is defined by

$$\left(-\frac{1}{2}\nabla^2 + U_M\right)\Phi_M^\gamma(\vec{r}) = -\frac{\gamma^2}{2}\Phi_M^\gamma(\vec{r}), \quad (2.2)$$

where γ represents a continuous parameter satisfying the condition $\phi \leq \gamma^2/2 \leq U_0$ [ϕ is the work function; see Fig. 1(b)]. Besides γ , the eigenstates $\Phi_M^\gamma(\vec{r})$ are specified by parabolic quantum numbers n_{1M} and m_M . For final state φ_A^{nl} we take

$$\varphi_A^{nl}(\vec{r}, t) = \Phi_{A, \gamma_{A0}}(\vec{r}_A) \exp\left[ivz - i\frac{v^2}{2}t + i\frac{\gamma_{A0}^2}{2}t\right], \quad (2.3)$$

where $\Phi_{A, \gamma_{A0}}$ is the hydrogenlike eigenstate of unit norm satisfying the relation

$$\left(-\frac{1}{2}\nabla^2 + U_A\right)\Phi_{A, \gamma_{A0}}(\vec{r}_A) = -\frac{\gamma_{A0}^2}{2}\Phi_{A, \gamma_{A0}}(\vec{r}_A). \quad (2.4)$$

In agreement with beam-foil measurements, the quantum numbers n and l and the magnetic quantum number m_A will be associated with $\Phi_{A, \gamma_{A0}}$. Consequently $\gamma_{A0} = Z/n$.

The corresponding transition amplitude $f(t)$ at time $t \rightarrow \infty$ is given by

$$f = \lim_{t \rightarrow \infty} \langle \varphi_A^{nl}(\vec{r}, t) | U(0, t) | \Phi_M^\gamma(\vec{r}) \rangle, \quad (2.5)$$

where $U(t_1, t_2)$ denotes the evolution operator of the system from time t_1 to t_2 . The last expression can be transformed in a more suitable form by introducing two important solutions (Ψ_M^γ and Ψ_A^{nl}) of the time-dependent Schrödinger equation $i(\partial\Psi/\partial t) = H\Psi$ and using the concept of the moving Firsov plane.¹⁰ For Ψ_M^γ we take an evolved initial state Φ_M^γ at time t , whereas Ψ_A^{nl} is an electron state at time t that will evolve in the moving atomic state φ_A^{nl} at $t \rightarrow \infty$,

$$\Psi_M^\gamma(\vec{r}, t) = U(0, t)\Phi_M^\gamma(\vec{r}), \quad (2.6a)$$

$$\Psi_A^{nl}(\vec{r}, t) = U(\infty, t)\varphi_A^{nl}(\vec{r}, \infty). \quad (2.6b)$$

The instantaneous position z_F of the S_F plane is defined by

$$z_F = R - a(t), \quad (2.7)$$

where $a = a(t)$ is the position of the S_F plane with respect to the moving projectile [see Fig. 1(b)].

A procedure explicated in Ref. 10 leads to the following expression for f :

$$f = \int_0^\infty I(t) dt, \quad (2.8a)$$

where

$$I(t) = \frac{i}{2} \int_{S_F} \left[\frac{\nabla\Psi_M^\gamma}{\Psi_M^\gamma} - \frac{\nabla\Psi_A^{nl*}}{\Psi_A^{nl*}} - 2iv \left(1 - \frac{da}{dR} \right) \vec{e}_z \right] \times \Psi_A^{nl*} \Psi_M^\gamma d\vec{S} \quad (2.8b)$$

is a (mixed) electron flux through the moving Firsov plane S_F . The unit vector \vec{e}_z is directed along the z axis of the system S , whereas $d\vec{S} = -dS \vec{e}_z$. Note that the transition amplitude f is determined by the time evolution of $\Psi_M^\gamma(\vec{r}, t)$ and $\Psi_A^{nl}(\vec{r}, t)$ exclusively on the S_F plane. Also, it is important to note that

$$I(t) = I \left[a, \frac{da}{dR}; t \right]$$

is a functional of the Firsov plane position $a = a(t)$.

Let us denote by $T_{nl}^\gamma(t)$ the probability of electron transition from initial states of unit γ interval (around given γ) of the foil valence band to the ionic state (n, l) . This probability, determined by

$$T_{nl}^\gamma(t) = |f(t)|^2 = \left| \int_0^t I(t) dt \right|^2, \quad (2.9)$$

also represents a functional of $a = a(t)$.

Its asymptotic form ($t \rightarrow \infty$) can be used for the determination of the Firsov plane kinematics by variational requirement. Using the notation $T_{nl}^\gamma = T_{nl}^\gamma(\infty)$ we set

$$\frac{\delta T_{nl}^\gamma}{\delta a} = 0, \quad (2.10)$$

where $\delta a(0) = 0$ and $\delta a(\infty) = 0$. A general background of the determination of the Firsov plane position $a = a(t)$ by variational requirement is given in Ref. 10. We note only that the condition (2.10) is more general than $\delta f / \delta a = 0$, used in the theory of the ground hydrogen state formation. The variational requirement (2.10) does not exist in the Demkov-Ostrovskii model¹¹ of the charge-exchange process in ion-atom collisions. Since our evaluation of the transition amplitude f is essentially based on this model, it will be useful to comment on its relationship with the present molecular model of charge exchange in ion beam-foil interaction.

The following facts could elucidate this relationship. The cited paper¹¹ deals with the charge exchange at large impact parameter b . This circumstance removes the explicit presence of the kinematic parameter $a(t)$ from the integrand of the Demkov-Ostrovskii electron flux $I(t)$. For the same reason ($b \gg 1$) the integral $f = \int_0^\infty I(t) dt$ is very simple and can be calculated directly by means of the stationary phase method. Finally, the applied procedure of the calculation gives a final expression for f whose dependence on the S_F plane position is weak and very simple, and can definitely be removed by simple estimation.

Obviously, a large collisional parameter does not exist in the ion beam-foil transmission geometry, which clearly indicates that the Demkov-Ostrovskii method cannot be directly transferred to the present problem. The lack of the large collisional parameter leads us to the conclusion that, even in the approximation of large ion-surface distances R , a more general and more appropriate expression for integrand of $I(t)$ must explicitly contain the kinematic factor $a(t)$. Accordingly, we derived Eq. (2.8b) for $I(t)$ and, consequently, determination of the S_F plane kinematics becomes necessary. Thus, realizing that the stationary phase method does not operate successfully in our case, as well as that the nonphysical ambiguity of the

$a(t)$ -dependent expression for f must be removed, we proposed the variational condition (2.10).

In the considered asymptotic case ($t \rightarrow \infty$), the integral in Eq. (2.9) can be seen as a Laplace transform $\mathcal{L}[F(t)]$ of a function $F(t)$ defined by

$$I(t) = e^{-pt} F(t), \quad (2.11)$$

where the parameter p is real and time independent. Thus,

$$T_{nl}^\gamma = f f^* = \mathcal{L}(F^* * F), \quad (2.12a)$$

where

$$F^* * F = \int_0^t F^*(t-\tau) F(\tau) d\tau \quad (2.12b)$$

denotes the autoconvolution of F . Passing to the electron flux convolution $I^* * I$ we obtain

$$T_{nl}^\gamma = \int_0^\infty I^* * I dt. \quad (2.13)$$

Inserting (2.13) into (2.10) we obtain the Euler-Lagrange equation

$$\frac{\partial(I^* * I)}{\partial a} - \frac{d}{dR} \left[\frac{\partial(I^* * I)}{\partial(da/dR)} \right] = 0. \quad (2.14)$$

which will be used for determination of $a = a(t)$.

Some general and natural requirements can be imposed on the kinematics of the S_F plane. In the initial stages ($t \approx 0$) of the ion's escape from the solid surface ($R \rightarrow 0, a \rightarrow 0$) we take

$$a(R)/R \rightarrow 1, \quad R \rightarrow 0. \quad (2.15a)$$

As we shall see in Sec. IV A, the physically most important time interval (when the population of Rydberg states predominantly takes place) can be characterized by

$$a(R)/R \approx g = \text{const}, \quad (2.15b)$$

where $g \approx \frac{1}{2}$ and where R will represent a sufficiently large quantity. Finally, at extremely large ion-surface distances R ($R \rightarrow \infty, a \rightarrow \infty$) we take

$$a(R)/R \rightarrow 0, \quad R \rightarrow \infty. \quad (2.15c)$$

The conditions (2.15a) and (2.15c) will be used in the determination of the wave functions Ψ_A^{nl} and Ψ_M^γ , whereas the expression (2.15b) will be employed in the transition probability calculations.

The transition probability $T_{nl}^\gamma(t)$, Eq. (2.9), can be connected with the total electron transition probability $T_{nl}(t)$ from all states of the solid conduction band to the Rydberg (n, l) state. We take

$$T_{nl}(t) = \int \sum n^\gamma T_{nl}^\gamma(t) d\gamma, \quad (2.16)$$

where n^γ stands for the population number of the conduction-band states. By \int and \sum we denote the integration over γ values of the conduction band and the summation over corresponding quantum numbers n_{1M} and m_M , respectively. The corresponding final value ($t \rightarrow \infty$) of $T_{nl}(t)$ will be denoted by T_{nl} .

In the actual calculation of T_{nl} we will suppose that

only one electron transition channel [leading to the given (n, l) state] is open. However, during the ion's escape from the solid surface all other channels (leading to all free ionic states) are also open and they participate simultaneously in the electron pickup process. This means that the actual population probability P_{nl} of the (n, l) state (measured in beam-foil experiments) will be lower in comparison with $T_{nl} = T_{nl}(\infty)$. In other words, a connection between T_{nl} and P_{nl} can be established only in the framework of a multichannel formalism. Such a multistage approach, adopted for the population of Rydberg states, will be developed in our subsequent discussion (Secs. V A and V B).

In order to complete the formulation of the problem, we review briefly the main results of our quantum-mechanical treatment of the multichannel population process. To do this, it is suitable to distinguish the (n, l) ionic state (populated with the probability P_{nl}) from all other "background" ionic states $(n, l' \neq l)$ and $(n' \neq n, l')$. We denote by $\tilde{P}_{nl}(t)$ the population probability of the ionic state (n, l) , supposing that only level n exists. The notation $P_{n'l'}^{nl}(t)$ will be used for population probability of the "background" state $(n' \neq n, l')$ in the presence of (n, l) state. With the adopted notations, the actual population probability $P_{nl} = P_{nl}(\infty)$ of the (n, l) state (in the presence of all ionic states) will be determined by

$$P_{nl} = \tilde{P}_{nl} \left[1 - \sum_{n' \neq n} \sum_{l' \neq l} P_{n'l'}^{nl} \right], \quad (2.17)$$

where $\tilde{P}_{nl} = \tilde{P}_{nl}(\infty)$ and $P_{n'l'}^{nl} = P_{n'l'}^{nl}(\infty)$. We point out that the expression (2.17) holds exclusively in the approximation of small transition probabilities.

Under the mentioned condition, the probability \tilde{P}_{nl} can be determined directly from the simple rate equation

$$\frac{d\tilde{P}_{nl}(t)}{dt} = \Gamma_{nl}(t)[1 - \tilde{P}_{nl}(t)], \quad (2.18)$$

where $\Gamma_{nl}(t) = dT_{nl}(t)/dt$ denotes the corresponding transition rate. Equation (2.18), together with the initial condition $\tilde{P}_{nl}(0) = 0$, gives

$$\tilde{P}_{nl} = 1 - e^{-T_{nl}}, \quad (2.19)$$

where $T_{nl} = T_{nl}(\infty)$ is determined by Eq. (2.16). Determination of the population probability $P_{n'l'}^{nl}$ of the background state (n', l') is more complicated. We realize, however, that the actual population probability P_{nl} , Eq. (2.17), does not depend significantly on the details of the population mechanisms of the background states. This circumstance will enable us to estimate the value of $P_{n'l'}^{nl}$ as a product of the probability $\tilde{P}_{n'l'}$ and a statistical factor $p_{n'l'}^{nl} \approx 1/n'$ (Sec. V B).

From the presented formulation of the problem we see that our further considerations will go through the following three steps. In the first step (Sec. III) we calculate the relevant wave functions $\Psi_A^{nl}(\vec{r}, t)$ and $\Psi_M^l(\vec{r}, t)$, appearing in the expression (2.8b) for the electron-density flux. In the second step (Sec. IV) we will use the obtained functions for the determination of the transition probability T_{nl} [Eq. (2.16) for $t \rightarrow \infty$]. Finally, in the third step

(Sec. V) we shall develop the multichannel theory of the Rydberg state population (calculating explicitly the background level population probabilities $P_{n'l'}^{nl}$), which will enable us to find the actual population probabilities P_{nl} .

III. CALCULATIONS OF Ψ_A^{nl} AND Ψ_M^l

The calculations of Ψ_A^{nl} and Ψ_M^l on the Firsov plane S_F are somewhat similar to those presented previously in our analysis of the population of the ground hydrogen state.¹⁰ In this section only specific features of this procedure (connected with the conditions $Z \approx n$, $n \gg 1$, and $l \ll n$) will be discussed in more detail.

A. The Ψ_A^{nl} function

The time-dependent wave function $\Psi_A^{nl}(\vec{r}, t)$ on the Firsov plane S_F can be obtained starting from the energy eigenproblem of the Hamiltonian H , Eq. (2.1). Namely, for a fixed (and large) ion-surface distance R we set

$$\left[-\frac{1}{2}\nabla^2 + U_A + (U_M + U_{AM}) \right] \Phi_{AM}(\vec{r}, R) = E_A(R) \Phi_{AM}(\vec{r}, R), \quad (3.1)$$

where the molecularlike eigenstate Φ_{AM} can be considered as the atomic eigenfunction $\Phi_{A, \gamma_{A0}}$ [Eq. (2.4)], distorted by the potential $U_M + U_{AM}$. We take

$$\Phi_{AM}(\vec{r}, R) = \Phi_{A, \gamma_{A0}}(\vec{r}_A) e^{-s_A(\vec{r}_A, R)}, \quad (3.2a)$$

where s_A represents a small correction. In the vicinity of the ionic core the Φ_{AM} function becomes $\Phi_{A, \gamma_{A0}}$. In that region we have

$$U_M + U_{AM} \approx \frac{2Z-1}{4R}$$

and

$$E_A(R) = -\frac{\gamma_A^2(R)}{2} \approx -\frac{\gamma_{A0}^2}{2} + \frac{2Z-1}{4R}, \quad (3.2b)$$

where all terms of order $O(1/R^2)$ are omitted. A typical position of the $E_A(R)$ -level is presented in Fig. 1(b).

In the moving coordinate system S' we use the following form of the relevant time-dependent wave function of the active electron:

$$\Psi_A^{nl}(\vec{r}_A, t) = \Phi_{AM}(\vec{r}, R) e^{f_A(\vec{r}_A, t)} e^{(i/2)\gamma_{A0}^2 t}, \quad (3.3)$$

where $R = vt$. The function f_A is an appropriate space-time correction satisfying the following condition at $t \rightarrow \infty$:

$$f_A(\vec{r}_A, t) \rightarrow 0, \quad t \rightarrow \infty. \quad (3.4)$$

We recall that for $t \rightarrow \infty$ both $a = a(t)$ and R tend to infinity, but $a/R \rightarrow 0$ [see Eq. (2.15c)]. Now, passing to the fixed coordinate system S we have

$$\Psi_A^{nl}(\vec{r}, t) = \Psi_A^{nl} e^{ivz - i(v^2/2)t}. \quad (3.5)$$

Looking at Eqs. (3.5), (3.3), and (3.2a) we see that the calculation of Ψ_A^{nl} is reduced to the evaluation of s_A and

f_A . A quasiclassical method^{10,11} giving s_A and f_A is briefly reviewed in the Appendix. In the central part of the S_F plane we obtain

$$s_A = -\frac{2Z-1}{4\gamma_{A0}} \frac{a}{R} + \frac{1}{4\gamma_{A0}} \ln \left[1 - \frac{a}{R} \right] - \frac{Z}{\gamma_{A0}} \ln \left[1 - \frac{a}{2R} \right] + s_{A0}, \quad (3.6)$$

where s_{A0} represents an arbitrary integration constant for a while. For f_A we have (in the same central region of the S_F plane)

$$f_A = -\frac{2Z-1}{4\gamma_{A0}} \frac{a}{R} + \frac{1}{4} \left[\frac{1}{\gamma_{A0}} - \frac{1}{\gamma_{A0}+iv} \right] \ln \left[1 - \frac{a}{R} \right] - Z \left[\frac{1}{\gamma_{A0}} - \frac{1}{\gamma_{A0}+2iv} \right] \ln \left[1 - \frac{a}{2R} \right]. \quad (3.7)$$

Let us note that the last expression does not contain any arbitrary integration constant.

The unknown constant s_{A0} in Eq. (3.6) can be calculated by using the form of $\Psi_{A'}^{nl}(\vec{r}_A, t)$ in the adiabatic limit (when $v \rightarrow 0$ and $R \approx \text{const}$). In this way we obtain (see Appendix)

$$s_{A0} \approx -\frac{2Z-1}{2\gamma_{A0}} \frac{a}{R} + i \frac{2Z-1}{4v}. \quad (3.8)$$

In the subsequent discussions the imaginary part of s_{A0} plays the role of an unimportant phase factor, so that it can be neglected.

In order to include the mentioned specific features of the problem considered here ($Z \approx n$, $n \gg 1$, and $l \ll n$), the hydrogenlike eigenfunction $\Phi_{A, \gamma_{A0}}$ must be treated more carefully. [This function appears in Eq. (3.2a) and, consequently, in Eqs. (3.3) and (3.5).] Expressing $\Phi_{A, \gamma_{A0}}$ in spherical coordinates r_A , Θ_A , and φ_A we obtain

$$\Phi_{A, \gamma_{A0}} = \mathcal{R}_{nl}(r_A) Y_l^{m_A}(\Theta_A, \varphi_A),$$

where the generalized Laguerre polynomial of the radial part \mathcal{R}_{nl} is given by

$$L_{n-l-1}^{2l+1}(x) = \frac{(n+l)!}{(n-l-1)!} (-x)^{n-l-1} S_{nl}(x). \quad (3.9a)$$

In writing the last expression we used the notations $x = 2\gamma_{A0} r_A$ and

$$S_{nl}(x) = \sum_{k=0}^{n-l-1} \frac{(-1)^k}{k!} \frac{(n+l)!(n-l-1)!}{(n+l-k)!(n-l-1-k)!} \left[\frac{1}{x} \right]^k. \quad (3.9b)$$

Note that in the case of low-lying states ($n \approx 1$) and far from the ionic core we have $S_{nl}(x) \approx 1 + O(1/x)$; for highly excited states ($n \gg 1$) this approximation breaks down.

So, for $n \gg 1$ another approximation for $S_{nl}(x)$ must be used. As we shall see, in the calculation of the electron-density flux I (Sec. IV) the function $\rho \Phi_{A, \gamma_{A0}}$ (ex-

pressed in polar coordinates ρ and φ) must be integrated over the S_F plane [see, e.g., Eq. (4.2)]. For the most relevant values of parameters describing the considered system ($Z \gg 1$, $n \approx Z$, $l \approx 0$ and $R \gg 1$), the mentioned integration can be simplified by taking

$$S_{nl}(x) \approx S_{nl}(4n) \quad (3.10)$$

for all x . This approximation allows us to continue further discussion on the analytic level. Its validity is supported by numerical calculations.

The spherical harmonics $Y_l^{m_A}$ can be simplified too. In the central region of the S_F plane we have $\rho \ll a$, so that

$$Y_l^{m_A} = (-1)^l \left[\frac{2l+1}{4\pi} \frac{(l-|m_A|)!}{(l+|m_A|)!} \right]^{1/2} \left[\frac{d^{|m_A|} P_l(y)}{dy^{|m_A|}} \right]_{y=1} \times \epsilon^{|m_A|/2} [1 + O(\epsilon)] e^{im_A \varphi}, \quad (3.11)$$

where $P_l(y)$ is Legendre polynomial, $y = \cos \Theta_A$, and $\epsilon = (\rho/a)^2 \ll 1$. Generally, in the calculation of the electron-density flux I through the S_F plane, all m_A sub-states of the (n, l) state must be included. But from Eq. (3.11) we see that the population of low-angular-momentum Rydberg states with $m_A = 0$ is dominant (since, in this case $\epsilon^{|m_A|/2} = 1$). Therefore, instead of (3.11) we can use the following approximation:

$$Y_l^{m_A} \approx (-1)^l \left[\frac{2l+1}{4\pi} \right]^{1/2} \delta_{m_A, 0}, \quad (3.12)$$

where $\delta_{m_A, 0}$ is the Kronecker symbol.

As a sufficient condition for the validity of (3.12) we can take

$$\frac{d^l P_l(y)}{dy^l} \epsilon^{1/2} \leq 1, \quad (3.13a)$$

i.e., taking that $\epsilon^{1/2} = \rho/a \sim 1/n$,

$$|2l-1|! \leq n. \quad (3.13b)$$

The last relation can serve as rough but sufficiently good estimation of the validity domain of the approximation. For example, if $n \approx Z = 7$ the applicability of our theory would be restricted to $l = 0, 1$, and 2 .

By using the explicit form of the radial part \mathcal{R}_{nl} of the function $\Phi_{A, \gamma_{A0}}$ and having in mind the approximate expressions (3.10) and (3.12), as well as Eqs. (3.2a), (3.6), and (3.8), we get

$$\Phi_{AM} \approx N_{A0} a^{Z/\gamma_{A0}-1} e^{-\gamma_{A0} r_A} \delta_{m_A, 0}, \quad (3.14a)$$

where

$$|N_{A0}| = \frac{\gamma_{A0}^2}{\sqrt{\pi Z}} (2\gamma_{A0})^{Z/\gamma_{A0}-1} e^{(2Z-1)/4\gamma_{A0}} \times \left[\frac{2l+1}{(n-l-1)!(n+l)!} \right]^{1/2} S_{nl}(4n). \quad (3.14b)$$

Note that Φ_{AM} states correspond to discrete points of the energy spectrum of the energy eigenproblem (3.1). Final-

ly, the time-dependent wave function $\Psi_A^{nl}(\vec{r}, t)$ on the S_F plane is determined by (3.5), (3.3), (3.7), and (3.14).

B. The Ψ_M^γ function

In calculating the time-dependent wave function $\Psi_M^\gamma(\vec{r}, t)$ we begin again with the energy eigenproblem of the Hamiltonian H at fixed (and large) R ,

$$\begin{aligned} [-\frac{1}{2}\nabla^2 + U_M + (U_A + U_{AM})]\Phi_{MA}^\gamma(\vec{r}, R) \\ = E_M(R)\Phi_{MA}^\gamma(\vec{r}, R), \end{aligned} \quad (3.15a)$$

where Φ_{MA}^γ belongs to the second class of the molecular-like eigensolutions. (Functions Φ_{AM} constitute the first class of those eigensolutions.) The function Φ_{MA}^γ is the metallic function Φ_M^γ [Eq. (2.2)], distorted by the potential $U_A + U_{AM}$; the eigenenergies $E_M(R)$ belong to the continuous negative energy spectrum. We adopt the following normalization condition:

$$\langle \Phi_{MA}^\gamma | \Phi_{MA}^{\gamma'} \rangle = \delta(\gamma - \gamma'). \quad (3.15b)$$

The energy eigenproblem (3.15a) will be solved by taking

$$\Phi_{MA}^\gamma(\vec{r}, R) = \Phi_M^\gamma(\vec{r}) e^{-s_M(\vec{r}, R)}, \quad (3.16a)$$

where $s_M(\vec{r}, R)$ is the corresponding space-correction factor of Φ_M^γ . In addition,

$$E_M(R) \approx -\gamma^2/2, \quad (3.16b)$$

where all terms of the order $O(1/R^2)$ are omitted. The time-dependent wave function $\Psi_M^\gamma(\vec{r}, t)$ is given by

$$\Psi_M^\gamma(\vec{r}, t) = \Phi_{MA}^\gamma(\vec{r}, R) e^{f_M(\vec{r}, t)} e^{i(\gamma^2/2)t}, \quad (3.17a)$$

where $R = vt$, whereas $f_M(\vec{r}, t)$ represents a small space-time correction factor of Φ_{MA}^γ satisfying the following initial condition:

$$f_M(\vec{r}, t) \rightarrow 0, \quad t \rightarrow 0. \quad (3.17b)$$

We recall that for $t \rightarrow 0$ both $a = a(t)$ and R tend to zero, but $a/R \rightarrow 1$, Eq. (2.15a).

For calculations of s_M and f_M we can use a method almost identical with those presented in the Appendix (see also Refs. 10 and 11). In the central part of the S_F plane we obtain

$$s_M = \frac{Z}{\gamma} \ln \left[\frac{a}{R} \right] + \frac{Z}{\gamma} \ln \left[2 - \frac{a}{R} \right] + s_{M0}, \quad (3.18)$$

where s_{M0} stands for an unknown integration constant. The function f_M is given by (in the central region of the S_F plane):

$$\begin{aligned} f_M = Z \left[\frac{1}{\gamma} - \frac{1}{\gamma + iv} \right] \ln \left[\frac{a}{R} \right] \\ + Z \left[\frac{1}{\gamma} - \frac{1}{\gamma - iv} \right] \ln \left[2 - \frac{a}{R} \right]. \end{aligned} \quad (3.19)$$

Therefore, in order to obtain $\Psi_M^\gamma(\vec{r}, t)$, Eq. (3.17a), it

remains to determine the explicit form of the function Φ_{MA}^γ . The expressions (3.16a) and (3.18) suggest that this problem could be reduced to the evaluation of Φ_M^γ and s_{M0} . However, we realized that it is more convenient to calculate the Φ_{MA}^γ function directly from Eq. (3.15a); moreover, an approximate solution of that kind is still known (see Ref. 10 and relevant references therein). In the cited papers, the Φ_{MA}^γ function has been obtained by JWKB method as an analytic continuation of the metallic function Φ_M^γ [Eq. (2.2), for $z < 0$ when $U_M = -U_0$] through the narrow cylindrical region around z axis into ionic region.

In the small central part of the S_F plane one obtains

$$\begin{aligned} \Phi_{MA}^\gamma = K^{MA}(R) \frac{\exp(im_M\varphi)}{\sqrt{\xi\eta}} M_{n_{1M} + (|m_M| + 1)/2, |m_M|/2}(\gamma\xi) \\ \times M_{\lambda_M, |m_M|/2}(\gamma\eta), \end{aligned} \quad (3.20a)$$

where $\xi = r_A + z_A$, $\eta = r_A - z_A$, and φ denote the parabolic coordinates in the moving coordinate system S' . By $M_{ab}(x)$ we denoted Whittaker functions (Ref. 13, p. 505) whereas

$$\lambda_M = \frac{Z}{\gamma} - \left[n_{1M} + \frac{|m_M| + 1}{2} \right]. \quad (3.20b)$$

The R -dependent factor $K^{MA}(R)$ is given by

$$K^{MA}(R) = K_{M0} R^{\lambda_M + 1/4\gamma} e^{-\gamma R}, \quad (3.20c)$$

where, denoting by $\Gamma(x)$ the gamma function,

$$\begin{aligned} |K_{M0}| = \frac{1}{\pi} \left[\frac{(|m_M| + n_{1M})!}{2(|m_M|!)^4 n_{1M}!} \right]^{1/2} \Gamma \left[-\lambda_M + \frac{|m_M| + 1}{2} \right] \\ \times \gamma^{\lambda_M + 1/2\gamma} (2e)^{1/4\gamma} 2^{\lambda_M - (2Z - 1)/2\gamma}. \end{aligned} \quad (3.20d)$$

In the considered electron pickup process, all m_M substates of the solid conduction band are not equally relevant. Namely, from the orthogonality of Φ_{MA}^γ and Φ_{AM} with respect to the angular variable φ we conclude that the transition probability will vanish for $m_A \neq m_M$ [see Eqs. (4.2) and (2.8a)]. On the other hand, considering the Φ_{AM} state we concluded that the ionic substates with $m_A = 0$ are dominant [see the discussion in connection with Eq. (3.11)]. Thus, the states Φ_{MA}^γ with $m_M = 0$ give the main contribution to the electron transitions.

For the Whittaker functions appearing in Eq. (3.20a) we can use corresponding asymptotic forms. In the central part of S_F plane ($\rho \rightarrow 0$) we have $\xi \rightarrow 0$; so, taking $m_M = 0$, we have (Ref. 13, p. 508)

$$M_{n_{1M} + 1/2, 0}(\gamma\xi) \approx \sqrt{\gamma\xi}. \quad (3.21a)$$

On the other hand, the variable $\gamma\eta \sim 2\gamma a$ of the second Whittaker function in Eq. (3.20a) is sufficiently large [for large R and, consequently, large a , see Eq. (2.15a)]. Thus, taking again $m_M = 0$ we have (Ref. 13)

$$M_{\lambda_M, 0}(\gamma\eta) \approx \frac{1}{\Gamma(-\lambda_M + \frac{1}{2})} (\gamma\eta)^{-\lambda_M} e^{\gamma\eta/2}, \quad (3.21b)$$

where the exponentially small terms are neglected.

Inserting Eqs. (3.21a) and (3.21b) into Eq. (3.20a) we obtain

$$\Phi_{MA}^\gamma \approx N_{M0} R^{Z/\gamma - n_{1M} - 1/2 + 1/4\gamma} a^{-Z/\gamma + n_{1M}} e^{-\gamma z}, \quad (3.22a)$$

where

$$|N_{M0}| = \frac{1}{\pi\sqrt{2}} \gamma^{1/2\gamma + 1/2} 2^{1/2\gamma - Z/\gamma - 1/2} (2e)^{1/4\gamma}. \quad (3.22b)$$

Concluding, the time-dependent wave function $\Psi_M^\gamma(\vec{r}, t)$ on the S_F plane is determined by Eqs. (3.17a), (3.19), and (3.22).

IV. CALCULATION

OF THE TRANSITION PROBABILITY T_{nl}

The functions Ψ_A^{nl} and Ψ_M^γ are, essentially, functionals of the Firsov plane position $a(t)$. Therefore, our first task is to find the function $a = a(t)$ by means of Eq. (2.14). After this we can pass to the explicit evaluation of the transition probability T_{nl} .

A. Kinematics of the Firsov plane S_F

In order to apply the Euler-Lagrange equation (2.14) it is necessary to have, first of all, an explicit form of the electron-density flux functional

$$I = I \left[a, \frac{da}{dR}, t \right],$$

given by Eq. (2.8b). An asymptotic approach is possible in the calculations of the terms $\nabla\Psi_M^\gamma/\Psi_M^\gamma$ and $\nabla\Psi_A^{nl}/\Psi_A^{nl}$ appearing in Eq. (2.8b): for large R we can assume that the S_F plane is sufficiently far from both solid surface and the ionic core. In that case, in the vicinity of S_F plane we have

$$\Psi_M^\gamma \sim e^{-\gamma z}, \quad \Psi_A^{nl} \sim e^{-\gamma A_0 r_A + i\omega z}, \quad (4.1)$$

which simplifies the calculation of the cited terms. On the other hand, describing the position of a point on the S_F plane by polar coordinates ρ and φ we have $dS = \rho d\rho d\varphi$ and $r_A = \sqrt{\rho^2 + a^2}$. Therefore, having in mind Eqs. (3.5) and (3.17a), we get

$$I \left[a, \frac{da}{dR}, t \right] = \frac{i}{2} e^{i\omega t} \left[\gamma + \gamma_{A0} + iv \left[1 - 2 \frac{da}{dR} \right] \right] \times \int_0^{2\pi} \int_0^\infty \Phi_{AM}^* \Phi_{MA}^\gamma e^{f_A^* + f_M} \rho d\rho d\varphi, \quad (4.2)$$

where

$$\omega = \frac{1}{2}(\gamma^2 - \gamma_{A0}^2)^2 - \frac{1}{2}v^2 \left[1 - 2 \frac{a}{R} \right]. \quad (4.3)$$

The integrand appearing in (4.2) can be simplified since only the central part of S_F plane contributes (in the case of the population of low-angular-momentum Rydberg states). Thus, using (3.14a) and (3.22a) we obtain

$$\rho \Phi_{AM}^* \Phi_{MA}^\gamma e^{f_A^* + f_M} \approx N(R) e^{-\gamma(R-a)} \rho e^{-\gamma_{A0} \sqrt{\rho^2 + a^2}}, \quad (4.4a)$$

where

$$N(R) = N_0 R^{Z/\gamma_{A0} - 3/2 + 1/4\gamma} \quad (4.4b)$$

and

$$N_0 = N_{A0}^* N_{M0} \left[\frac{a}{R} \right]^{Z/\gamma_{A0} - Z/\gamma + n_{1M} - 1} \times e^{f_A^* + f_M} \delta_{m_A, 0} \delta_{m_A, m_M}. \quad (4.4c)$$

Inserting (4.4) into (4.2) and performing an integration we get the following explicit expression for the electron-density flux functional:

$$I \left[a, \frac{da}{dR}, t \right] = \frac{i\pi e^{i\omega t}}{\gamma_{A0}^2} N(R) \left[\gamma + \gamma_{A0} + iv \left[1 - 2 \frac{da}{dR} \right] \right] \times (1 + \gamma_{A0} a) e^{-\gamma(R-a) - \gamma_{A0} a}, \quad (4.5)$$

where $R = vt$.

Now, for an approximate but analytic calculation of the convolution $I^* * I$, appearing in (2.14), we take

$$a(R) = g(R) R. \quad (4.6)$$

As we shall see in Sec. IV B, the electron-capture process dominantly takes place in a region of ionic trajectory where the ion-surface distance R is close to the critical distance R_c , Eq. (4.23b). In the interaction region we can assume that the kinematic factor $g(R)$, defined by Eq. (4.6), represents a weakly R -dependent function.

Having in mind the mentioned approximations, we obtain the following expression for electron-density flux convolution:

$$I^* * I = C \left[(\gamma + \gamma_{A0})^2 + v^2 \left[1 - 2 \frac{da}{dR} \right]^2 \right] I_g(g) I_a(a) \times a^{2\bar{\alpha} + 2} R^{2(\alpha - \bar{\alpha}) + 1} e^{(\gamma - \gamma_{A0})a} e^{-\gamma R}, \quad (4.7)$$

where

$$C = \frac{1}{v} \frac{\pi^2}{\gamma_{A0}^2} |N_{A0}|^2 |N_{M0}|^2 \delta_{m_A, 0} \delta_{m_A, m_M} \quad (4.8a)$$

and

$$\alpha = \frac{Z}{\gamma_{A0}} - \frac{3}{2} + \frac{1}{4\gamma}, \quad (4.8b)$$

$$\bar{\alpha} = \frac{Z}{\gamma_{A0}} - \frac{Z}{\gamma} + n_{1M} - 1 \quad (4.8c)$$

are R -independent quantities. The functions $I_g(g)$ and $I_a(a)$ are determined by

$$I_g(g) = \exp\{2 \operatorname{Re}[f_A^*(g) + f_M(g)]\}, \quad (4.9a)$$

$$I_a(a) = \frac{1}{\sqrt{2\pi}} \frac{B(\alpha+2, \alpha+2) \Gamma(\alpha + \frac{3}{2})}{(\alpha + \frac{3}{2})^{\alpha+2}} e^{\alpha+3/2} \times \left[1 + O\left(\frac{1}{a}\right) \right], \quad (4.9b)$$

where $B(\alpha+2, \alpha+2)$ stands for the beta function.

Using Eq. (4.7) we obtain the following expression for the first term on the left-hand side of Euler-Lagrange equation (2.14):

$$\frac{\partial(I^{**}I)}{\partial a} = \left[\frac{1}{R} \left[\frac{1}{I_g} \frac{dI_g}{dg} \right] + \left[\frac{1}{I_a} \frac{dI_a}{da} \right] + \frac{2\bar{\alpha}+2}{a} + (\gamma - \gamma_{A0}) \right] (I^{**}I). \quad (4.10)$$

On the other hand, by using cited approximations (valid for the interaction region) we get

$$\frac{d}{dR} \left[\frac{\partial(I^{**}I)}{\partial(da/dR)} \right] \approx u(p) \frac{\partial(I^{**}I)}{\partial R} + pu(p) \frac{\partial(I^{**}I)}{\partial a}, \quad (4.11)$$

where $p = da/dR$ and

$$u(p) = - \frac{4v^2(1-2p)}{(\gamma + \gamma_{A0})^2 + v^2(1-2p)^2}. \quad (4.12)$$

The derivative $\partial(I^{**}I)/\partial R$, appearing in (4.11), is given by

$$\frac{\partial(I^{**}I)}{\partial R} = \left[-\frac{a}{R^2} \left[\frac{1}{I_g} \frac{dI_g}{dg} \right] + \frac{2(\alpha - \bar{\alpha}) + 1}{R} - \gamma \right] \times (I^{**}I). \quad (4.13)$$

Inserting the expressions (4.10) and (4.11) into the Euler-Lagrange equation (2.14) we obtain

$$\frac{1 - pu(p)}{u(p)} = G(R), \quad (4.14)$$

where

$$g = \frac{a(R)}{R} = \frac{\gamma}{\gamma - \gamma_{A0}} \left[1 - \left\{ 1 + \frac{(\gamma - \gamma_{A0})^2}{\gamma^2} \left[\left[\frac{\gamma + \gamma_{A0}}{2v} \right]^2 - \frac{\gamma}{\gamma - \gamma_{A0}} + \frac{1}{4} \right] \right\}^{1/2} \right] \quad (4.20)$$

is an R -independent quantity. In the subsequent calculations of the transition probability T_{ni}^γ (Sec. IV B) we can assume that $a = gR$ is valid even for $R \gg R_c$ [since the integrand in (4.2) is an exponentially decreasing function of R].

Finally, let us note that the approximations used in the determination of Firsov plane kinematics do not affect the transition amplitude significantly. This is a direct consequence of the application of the variational requirement (2.10) in determination of $a = a(R)$. Small varia-

$$G(R) = \left[-\gamma + \frac{2(\alpha - \bar{\alpha}) + 1}{R} - \frac{a}{R^2} \left[\frac{1}{I_g} \frac{dI_g}{dg} \right] \right] \times \left[\gamma - \gamma_{A0} + \frac{2\bar{\alpha} + 2}{a} + \frac{1}{I_a} \frac{dI_a}{da} + \frac{1}{R} \left[\frac{1}{I_g} \frac{dI_g}{dg} \right] \right]^{-1}. \quad (4.15)$$

The last expression for $G(R)$ can be simplified, since the interaction region is sufficiently far from the solid surface (large $R \sim R_c$). In that case we have

$$\frac{1}{R} \left[\frac{1}{I_g} \frac{dI_g}{dg} \right] = O\left(\frac{1}{R}\right), \quad \frac{1}{I_a} \frac{dI_a}{da} = O\left(\frac{1}{R}\right) \quad (4.16)$$

so that, for $\gamma \neq \gamma_{A0}$,

$$G(R) \approx - \frac{\gamma}{\gamma - \gamma_{A0}} = G. \quad (4.17)$$

If $\gamma = \gamma_{A0}$ we obtain that $G(R) \sim a \sim R$.

Therefore, by using Eqs. (4.14) and (4.17) we obtain (for $\gamma \neq \gamma_{A0}$) the following quadratic equation for $p = da/dR$:

$$p^2 + 2Gp - \left[\left[\frac{\gamma + \gamma_{A0}}{2v} \right]^2 + G + \frac{1}{4} \right] = 0, \quad (4.18)$$

which leads to the differential equation

$$\frac{da}{dR} = -G \left[1 - \left\{ 1 + \frac{1}{G^2} \left[\left[\frac{\gamma + \gamma_{A0}}{2v} \right]^2 + G + \frac{1}{4} \right] \right\}^{1/2} \right]. \quad (4.19a)$$

If $\gamma = \gamma_{A0}$ we have

$$\frac{da}{dR} \approx \frac{1}{2}. \quad (4.19b)$$

Note that the last expression can be formally obtained from (4.19a) by taking $G \rightarrow \infty$. Thus, for our determination of Firsov plane kinematics Eq. (4.19a) can be used for both $\gamma \neq \gamma_{A0}$ and $\gamma = \gamma_{A0}$.

Extrapolating the validity domain of Eq. (4.19a) into the near surface region ($0 \leq R < R_c$) and using the initial condition $a \rightarrow 0, R \rightarrow 0$ we get $a = gR$, where

tions of $a = a(R)$ around a "true" stationary solution $\bar{a} = \bar{a}(R)$ of the variational equation (2.14) induce only small variations of the electron flux convolution $I^{**}I$.

B. Transition probability T_{ni}

We begin with the calculation of the time-dependent transition probability $T_{ni}^\gamma(t)$ defined by Eq. (2.9). Inserting Eq. (4.5), where $a/R = g$, into Eq. (2.9) we obtain

$$T_{nl}^{\gamma}(t) = |N_0|^2 \frac{\pi^2}{\gamma_{A0}^4} [(\gamma + \gamma_{A0})^2 + v^2(1-2g)^2] |J(t)|^2 \times \delta_{m_A,0} \delta_{m_A, m_M}. \quad (4.21)$$

The time-dependent quantity $J(t)$ is given by

$$J(t) = \int_0^t (1 + \gamma_{A0}gR) R^{\alpha} e^{-\Omega t} e^{i\omega t} dt, \quad (4.22a)$$

where $R = vt$. The α parameter is defined by Eq. (4.8b), whereas

$$\Omega = [\gamma(1-g) + \gamma_{A0}g]v. \quad (4.22b)$$

Note that the parameter ω appearing in (4.22a) is now a time-independent quantity.

Some evidence about the behavior of the integrand in Eq. (4.22a) follows from the analysis of its nonoscillatory part

$$j(R) = (1 + \gamma_{A0}gR) R^{\alpha} \exp\left[-\frac{\Omega}{v}R\right].$$

The function $j(R)$ has maximum at ion-surface distance R_m :

$$R_m = \frac{\alpha}{\gamma_{A0}g + \gamma(1-g)} \left[1 + O\left(\frac{1}{\alpha}\right)\right], \quad (4.23a)$$

where (in the case of Rydberg states) $\alpha \approx n \gg 1$. The oscillatory part $\exp[(i\omega/v)R]$ of the integrand in Eq. (4.22a) mainly cancels the contribution to the considered integral from the region around R_m . Thus, the physically most relevant R region of the integration in Eq. (4.22a) is shifted toward larger ion-surface distances, i.e., in the asymptotic region $R > R_c$ where

$$R_c \approx 2R_m. \quad (4.23b)$$

The relation (4.23b) supports the heuristic, quasiclassical arguments mentioned in the Introduction. Indeed, for a rough estimation of R_c by means of Eq. (4.23b) we take $\gamma \approx \gamma_{A0}$ and $g \approx \frac{1}{2}$, which gives $R_c \approx 2n^2/Z$. On the other hand, the length a_n of the major axis of the classical elliptic trajectory (in the direction of ionic motion) is approximately $2n^2/Z$. Thus, we have $R_c \approx a_n$, which indicates that the formation of Rydberg states with high eccentricity starts at those ion-surface distances R where the stable "classical" elliptic orbit of captured electron is possible.

The integral (4.22a) can be expressed (Ref. 13, p. 260) by the incomplete gamma function $\gamma(\nu, z)$:

$$J(t) = \frac{1}{v} \left[\frac{\gamma_{A0}g}{\beta^{\alpha+2}} \gamma(\alpha+2; \beta R) + \frac{1}{\beta^{\alpha+1}} \gamma(\alpha+1; \beta R) \right], \quad (4.24)$$

where $R = vt$ and $\beta = (\Omega - i\omega)/v$. Asymptotic behavior ($t \rightarrow \infty$, or $R \rightarrow \infty$) of $J(t)$ depends of $\text{Re}(\beta R) \gg 1$; using the asymptotic forms of $\gamma(\alpha+2, \beta R)$ and $\gamma(\alpha+1, \beta R)$ we obtain

$$|J(t)|^2 = v^{2\alpha} \Gamma^2(\alpha+1) \mathcal{A}(\gamma, v) |1 - \mathcal{B}(R)e^{-\beta R}|^2, \quad (4.25)$$

where

$$\mathcal{A}(\gamma, v) = \frac{[\gamma_{A0}g(\alpha+1)v + \Omega]^2 + \omega^2}{(\Omega^2 + \omega^2)^{\alpha+2}} \quad (4.26a)$$

and

$$\mathcal{B}(R) = \frac{1}{\Gamma(\alpha+1)} \left[1 + \frac{\gamma_{A0}g}{\gamma_{A0}g(1+\alpha) + \beta} \beta R \right] (\beta R)^{\alpha}. \quad (4.26b)$$

In the case of large R , the factor $\mathcal{B}(R)\exp(-\beta R)$ appearing in Eq. (4.25) can be neglected. In this way we obtain the following final expression for the transition probability $T_{nl}^{\gamma} = T_{nl}^{\gamma}(\infty)$:

$$T_{nl}^{\gamma} = |N_0|^2 \frac{\pi^2}{\gamma_{A0}^4} [(\gamma + \gamma_{A0})^2 + v^2(1-2g)^2] \times v^{2\alpha} \Gamma^2(\alpha+1) \mathcal{A}(\gamma, v). \quad (4.27)$$

For $|N_0|^2$ we have

$$|N_0|^2 = g^{2n_{1M}} |N_{A0}|^2 |N_{M0}|^2 \mathcal{N}^2(g), \quad (4.28a)$$

where $|N_{A0}|$ and $|N_{M0}|$ are defined by Eqs. (3.14b) and (3.22b), respectively, whereas

$$\begin{aligned} \mathcal{N}^2(g) &= g^{2Z/\gamma_{A0} - 2Z/\gamma - 2} (1-g)^{v^{2/2\gamma_{A0}}(\gamma_{A0}^2 + v^2)} \\ &\times \left[1 - \frac{g}{2}\right]^{-(8Zv^2/\gamma_{A0})(\gamma_{A0}^2 + 4v^2)} \\ &\times [g(2-g)]^{2Zv^2/\gamma(\gamma^2 + v^2)} e^{-(2Z-1)g/2\gamma_{A0}}. \end{aligned} \quad (4.28b)$$

The kinematic parameter g of the S_F plane is determined by Eq. (4.20).

From the obtained expression for T_{nl}^{γ} we can conclude that the whole n_{1M} dependence of T_{nl}^{γ} is contained in the factor $g^{2n_{1M}}$. Since the parameter g is approximately equal to $\frac{1}{2}$ (or somewhat greater than $\frac{1}{2}$) we see that T_{nl}^{γ} is a sufficiently strong decreasing function of n_{1M} . (Numerical tests show that T_{nl}^{γ} is nearly exponential function of n_{1M} : $T_{nl}^{\gamma} \sim e^{-n_{1M}}$.) This means that the conduction-band electrons with $n_{1M} = 0$ give a main contribution to the electron pickup process.

Further, from the expression (4.27) we can conclude that the considered process has nonresonant character (at intermediate velocities). This conclusion stems from the dynamic quantum model and it was not found in the quasistatic considerations.⁹ The appearance of the nonresonant electron transitions in the intermediate velocity region is transparent from the expression (4.27). Indeed, at very small velocities the function $\mathcal{A}(\gamma, v)$ is similar to Dirac's δ function (what indicates a resonant character of electron transitions in the quasistatic case). As v increases, the width of the $\mathcal{A}(\gamma, v)$ shape becomes larger and larger, so that at intermediate velocities the whole conduction band participates in the process.

Finishing with T_{nl}^{γ} we use Eq. (2.16) for the calculation of the probability $T_{nl} = T_{nl}(\infty)$ of transition from all

states of the solid conduction band. For the population number n^γ we shall take $n^\gamma=1$, which corresponds to the absolutely cold metal approximation. Recalling that the conduction-band state with $m_M=0$ give main contribution, we have

$$T_{nl} = \int_{\gamma_\phi}^{\gamma_{U_0}} \sum_{n_{1M}=0}^{\infty} T_{nl}^\gamma d\gamma, \quad (4.29)$$

where γ_ϕ and γ_{U_0} are determined by $\frac{1}{2}\gamma_\phi^2 = \phi$ and $\frac{1}{2}\gamma_{U_0}^2 = U_0$. The integration and summation in Eq. (4.29) requires numerical treatment; since T_{nl}^γ is a strongly decreasing function of n_{1M} , only a few terms in the sum are sufficient (we take $n_{1M}=0, 1, 2, 3$, and 4). The nonresonant character of the process is again evident from Fig. 2, where the γ dependence of the integral $\sum T_{nl}^\gamma$ is illustrated for $\nu=2$ a.u.

The work function ϕ for pure elemental graphite is, according to Ref. 14, about 5 eV. But, in the real experimental conditions (Refs. 1–8) foils contain impurities, which will result⁸ in the lowering of the work function ϕ . In the first numerical calculations^{6,7} based on the quasi-static model⁹ the value $\phi=4$ eV was adopted for comparison with experiments. The authors of those calculations also found some correlation with experiments for lower values of n , even if $\phi=3$ eV. However, strong instability of P_{nl} values with respect to ϕ have been found for higher n .

In the dynamic model presented in this paper the population probability P_{nl} does not depend strongly on ϕ ; moreover, P_{nl} can be assumed to be a weak function of ϕ . We found that $\phi=3$ eV fits best. In addition, in the dynamic model P_{nl} is remarkably stable with respect to U_0 ; we take $U_0=10$ eV as a “best” choice.

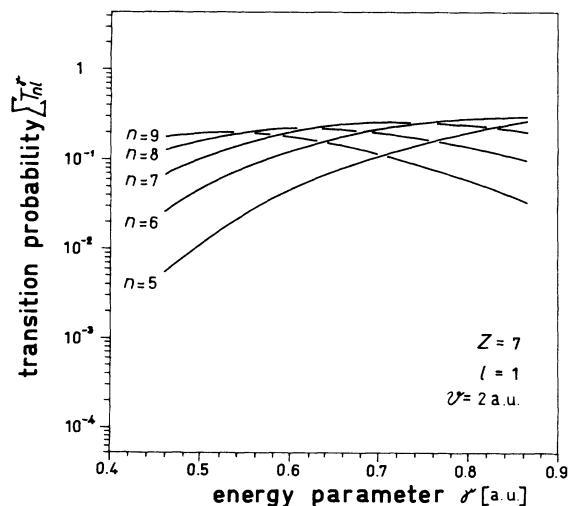


FIG. 2. γ dependence of the transition probability $\sum_{n_{1M}} T_{nl}^\gamma$, indicating the nonresonant character of the electron pickup in the intermediate velocity region.

V. CALCULATION OF THE POPULATION PROBABILITY P_{nl}

The expression (2.17) for P_{nl} can be obtained in the framework of a multichannel quantum-mechanical formalism. At the same time, this formalism will justify the use of Eq. (2.19).

A. Multichannel treatment of the Rydberg state population process

Our approach to the multichannel population of Rydberg states will be somewhat similar to the statistical treatment of the radiative decay in the ensemble of excited atoms, being initially in a mixed state (see, e.g., Ref. 15). Our first task, therefore, will be to construct an appropriate time-dependent statistical operator $\rho(t)$ describing the statistical mixture of relevant solid and ionic one-electron states. After that, the population probability P_{nl} can be related in the standard way with quantum transitions from the mixed state $\rho(t)$ to the moving ionic state $\varphi_A^{nl}(t)$ at $t \rightarrow \infty$.

In order to define the operator $\rho(t)$, we need, first of all, an appropriate set of one-electron wave functions that takes into account the presence of all open transition channels. Let us note that the set of metalliclike functions $\Psi_M^\gamma(t)$, Eq. (2.6a), does not satisfy this requirement: these functions represent states evolved from γ eigenstates Φ_M^γ , exclusively in the presence of only one ionic state (n, l) . Contributions of all other open channels leading to the “background” ionic states $(n, l' \neq l)$ and $(n' \neq n, l')$ of the state (n, l) , can be taken into account by using the following wave function:

$$\begin{aligned} \psi_{nl}^\gamma(t) = & \Psi_M^\gamma(t) e^{-T_{nl}^\gamma(t)/2} + \sum_{l' \neq l} a_{nl'l'}^\gamma(t) \varphi_A^{n'l'}(t) \\ & + \sum_{n' \neq n} \sum_{l'=0}^{n'-1} a_{n'l'l'}^\gamma(t) \varphi_A^{n'l'}(t), \end{aligned} \quad (5.1)$$

where $a_{nl'l'}^\gamma(t)$ and $a_{n'l'l'}^\gamma(t)$ are time-dependent expansion coefficients. The quantity $T_{nl}^\gamma(t)$ is the transition probability per unit γ from the state Ψ_M^γ to the moving ionic state φ_A^{nl} , Eq. (2.9).

Generally, in the case of the selective population of Rydberg states, all probabilities are very small so that the condition $T_{nl}^\gamma(t) \ll 1$ will be used. Thus, the first term in Eq. (5.1) describes the slow decay of the state $\Psi_M^\gamma(t)$ into ionic state φ_A^{nl} , in the absence of the background ionic states. All other terms in Eq. (5.1) take into account the influence of the background channels during the mentioned slow decay of the state $\Psi_M^\gamma(t)$. For the state $\Psi_M^\gamma(t)$ we adopted the normalization

$$\langle \Psi_M^\gamma(t) | \Psi_M^{\gamma'}(t) \rangle \approx \langle \Phi_{MA}^\gamma | \Phi_{MA}^{\gamma'} \rangle = \delta(\gamma - \gamma')$$

[see Eq. (3.15b)].

The corresponding statistical operator $\rho(t)$ has the form

$$\rho(t) = \int n^\gamma |\psi_{nl}^\gamma(t)\rangle \langle \psi_{nl}^\gamma(t)| d\gamma, \quad (5.2)$$

where n^γ are the population numbers of the solid conduction-band states. To simplify notation, in Eq. (5.2)

we omitted summations $\sum_{n_{1M}}$ and \sum_{m_M} with respect to the conduction-band quantum numbers n_{1M} and m_M . In the adopted notation, the population number n^γ satisfies the condition $\int n^\gamma d\gamma = \Gamma$, where $\Gamma = \gamma_{U_0} - \gamma_\phi$. This condition agrees with the absolute cold metal approximation; see comment followed by Eq. (4.29).

For the actual population probability $P_{nl}(t)$ of the ionic state (n, l) we have

$$P_{nl}(t) = \frac{\text{Tr}[\rho(t)|\varphi_A^{nl}(t)\rangle\langle\varphi_A^{nl}(t)|]}{N^{-1}\text{Tr}\rho(t)}, \quad (5.3)$$

where N stands for the total number of the solid conduction electrons. Of course, the appearance of the denominator $N^{-1}\text{Tr}\rho(t)$ in Eq. (5.3) results from the adopted normalization conditions of the state Ψ_M^γ and the population number n^γ . The expressions (5.3), (5.2), and (5.1) complete the general basis of our multichannel treatment of the Rydberg states population process.

By using the standard eigendifferential technique of trace calculations (see, for example, Ref. 16) and having in mind the mentioned approximation of small transition probabilities we obtain

$$P_{nl}(t) = \tilde{P}_{nl}(t) \left[1 - \sum_{n' \neq n} \sum_{l'=0}^{n'-1} P_{n'l'}^{nl}(t) + O((T_{nl})^2) \right], \quad (5.4)$$

where $\tilde{P}_{nl}(t)$ represents the population probability of the ionic (n, l) state in the presence of the background states $(n, l' \neq l)$. The contributions of remaining background channels are described by the population probability $P_{n'l'}^{nl}(t)$ of the state $(n' \neq n, l')$ in the presence of open channels $\gamma \rightarrow (n, l)$, where $\gamma_\phi < \gamma < \gamma_{U_0}$.

The probability $\tilde{P}_{nl}(t)$ can be obtained from Eqs. (5.3) and (5.2) providing that we take $a_{n'l'}^\gamma(t) = 0$ for $n' \neq n$ in the expression (5.1). We get

$$\tilde{P}_{nl}(t) = T_{nl}(t) \left[1 - \sum_{l' \neq l} \tilde{T}_{nl'}^{nl}(t) + O((T_{nl})^2) \right], \quad (5.5)$$

where

$$\tilde{T}_{nl'}^{nl}(t) = \int n^\gamma p_{n'l'}^{\gamma nl}(t) T_{n'l'}^\gamma(t) d\gamma \quad (5.6a)$$

and

$$p_{n'l'}^{\gamma nl}(t) = \frac{e^{T_{nl'}^\gamma(t)}}{NT_{n'l'}^\gamma} \{ 2 \text{Re}[a_{n'l'}^\gamma(t) \langle \Psi_M^\gamma(t) | \varphi_A^{nl}(t) \rangle] \times e^{-T_{nl'}^\gamma(t)/2} + |a_{n'l'}^\gamma(t)|^2 \}. \quad (5.6b)$$

For the transition probability $T_{n'l'}^\gamma$ the expression (2.9) holds, where we set l' instead of l .

The population probability $P_{n'l'}^{nl}(t)$, appearing in the sum of Eq. (5.4), is given by

$$P_{n'l'}^{nl}(t) = \int n^\gamma p_{n'l'}^{\gamma nl}(t) \tilde{P}_{n'l'}^\gamma(t) d\gamma, \quad (5.7)$$

where $p_{n'l'}^{\gamma nl}(t)$ is defined by (5.6b) providing that the set of indices (n, l') is replaced by (n', l') . For the probability $\tilde{P}_{n'l'}^\gamma$, appearing in the integrand of Eq. (5.7), we have

$$\tilde{P}_{n'l'}^\gamma(t) = T_{n'l'}^\gamma(t) [1 + O(T_{n'l'})]. \quad (5.8a)$$

The population probability $\tilde{P}_{n'l'}(t)$ of the (n', l') -background state in the presence of remaining $(n', l' \neq l')$ states of the ionic level $n' \neq n$ is determined by

$$\tilde{P}_{n'l'}(t) = \int n^\gamma \tilde{P}_{n'l'}^\gamma(t) d\gamma. \quad (5.8b)$$

Inserting (5.8a) into (5.8b) we arrive directly to expressions almost identical with Eqs. (5.5), (5.6a), and (5.6b): instead of n, l , and l' we must take n', l' , and l'' , respectively. In other words, these relations can be used not only for calculation of \tilde{P}_{nl} but also for determination of $\tilde{P}_{n'l'}$ where $n' \neq n$ [see Eq. (5.12)].

From Eqs. (5.5) and (5.6a) as well as (5.7) and (5.8a) we conclude that the actual population probability $P_{nl}(t)$ of the ionic state (n, l) , Eq. (5.4), is expressed completely in terms of the one-channel transition probabilities $T_{n'l'}^\gamma(t)$ and $T_{n'l'}^{\gamma nl}(t)$. The interference of channels is described exclusively by the time-dependent factors $p_{n'l'}^{\gamma nl}(t)$. In other words, the presented formalism and the proposed approximation of small transition probabilities enabled us to "localize" the complexity of the multichannel electron transitions in these factors.

B. Population probability P_{nl}

The obtained quantum-mechanical expression (5.4) for P_{nl} can be simplified when the transition probabilities are sufficiently small quantities. In that case, the higher-order terms in Eq. (5.4) can be omitted and we arrive just to the "classical" law of the probability composition, Eq. (2.17). Let us note, however, that even in the proposed approximation the expression for P_{nl} contains the unknown functions $p_{n'l'}^{\gamma nl}(t)$ of an exclusively quantum-mechanical nature.

It is quite transparent that the determination of these functions is connected with the very complex time-evolution problem of the $\psi_{nl}^\gamma(t)$ state; see Eqs. (5.6b) and (5.1). In addition, it is reasonable to expect that "true" values of $p_{n'l'}^{\gamma nl}(t)$ will be very complicated functions of the ionic quantum numbers and parameter γ . Therefore, it is practically impossible to continue our discussion without introducing some additional plausible arguments.

One possible way to overcome this problem is based on the supposition that the probability P_{nl} does not depend significantly on details on the background channels activity. In that case, we found that the factors $p_{n'l'}^{\gamma nl}(t)$ for fixed n and l can be considered (at $t \rightarrow \infty$) as stochastic functions of γ and l' so that some appropriate averaged values of these functions with respect to γ and l' can be used. In addition, for the population of Rydberg states we supposed that these averaged values, denoted by $p_{n'l'}^{nl}$, are sufficiently small quantities.

Looking for an appropriate expression for $p_{n'l'}^{nl}$ we realized that the following simple formula can be used: $p_{n'l'}^{nl} \approx 1/n'$. Obviously, the use of $p_{n'l'}^{nl} \approx 1/n'$ in the expression (5.4) for the transition probability P_{nl} leads to the corresponding relation which describes the population process in terms of decoupled channels. In that case, the values $p_{n'l'}^{nl}$ appear as statistical weights of those channels. As we shall see, the estimation $p_{n'l'}^{nl} \approx 1/n'$ leads to

an approximate but sufficiently good final expression for P_{nl} , which reproduces all available experimental facts. Some additional (theoretical) consequences supporting the plausibility of the proposed estimation will be mentioned at the end of this section; see the discussion followed by Eq. (5.14).

The proposed values of p_n^{nl} lead us to the "classical" connection between \tilde{P}_{nl} and T_{nl} described by the solution (2.19) of the rate equation (2.18). Namely, the expression (5.5) for \tilde{P}_{nl} at $t \rightarrow \infty$ can be rewritten as

$$\tilde{P}_{nl} = T_{nl} [1 - \langle T_{n'l'} \rangle_{l'}], \quad (5.9)$$

where higher-order terms with respect to T_{nl} are omitted, and where

$$\langle T_{n'l'} \rangle_{l'} = \frac{1}{n-1} \sum_{l' \neq l} T_{n'l'}. \quad (5.10)$$

This arithmetic mean of $T_{n'l'}$, taken over all background states ($n, l' \neq l$) of the level n can be calculated numerically by using Eq. (4.29) for $T_{n'l'}$. We found that in the case of small angular momentum l and for $n \approx Z$ the following approximation holds: $\langle T_{n'l'} \rangle_{l'} \approx \frac{1}{2} T_{nl}$. Thus,

$$\tilde{P}_{nl} = T_{nl} - \frac{1}{2} T_{nl}^2 + \dots \approx 1 - e^{-T_{nl}}, \quad (5.11)$$

which is just the mentioned solution (2.19) of the rate equation (2.18) for $t \rightarrow \infty$.

Inserting the averaged value p_n^{nl} into Eq. (5.7) and omitting the higher-order terms in Eq. (5.4) we obtain, at $t \rightarrow \infty$,

$$P_{nl} = \tilde{P}_{nl} \left[1 - \sum_{n' \neq n} \langle \tilde{P}_{n'l'} \rangle_{l'} \right], \quad (5.12)$$

where $\langle \tilde{P}_{n'l'} \rangle_{l'}$ denotes the arithmetic mean of $\tilde{P}_{n'l'}$ with respect to l' ; see Eq. (5.8b). It is not necessary to take into account contributions of all terms in the sum $\sum_{n' \neq n} \langle \tilde{P}_{n'l'} \rangle_{l'}$: only the background levels n' , positioned in the neighborhood of the level n , participate significantly. We found by direct numerical calculation that $\langle \tilde{P}_{n'l'} \rangle_{l'} \approx \tilde{P}_{n'l'=1}$, when $n' \approx n \approx Z$. Therefore, considering $\tilde{P}_{n'l'=1}$ as sufficiently small quantity, we get

$$P_{nl} = \tilde{P}_{nl} \prod_{n' \neq n} (1 - \tilde{P}_{n'l'=1}) \quad (5.13)$$

or

$$P_{nl} = (1 - e^{-T_{nl}}) \exp \left[- \sum_{n' \neq n} T_{n'l'=1} \right], \quad (5.14)$$

where T_{nl} and $T_{n'l'=1}$ are given by Eq. (4.29). The last relation is our final expression for P_{nl} , which will be compared with experimental data.

The obtained relation (5.14) can be considered as a generalization of the adiabatic formula $P_{nl} = 1 - \exp(-\text{const}/v)$, used in the quasistatic model.⁹ A comparison of these two formulas can elucidate the background of limitations of the quasistatic model in the Rydberg state population problem. Namely, the two-state character of the quasistatic approach reduces formally to the condition $T_{n'l'=1} = 0$. Besides, the adiabatic character of the mentioned model⁹ means essentially that the

more complex, nonmonotonic v dependence of $T_{nl} = T_{nl}(v)$ is simplified by taking $T_{nl} = \text{const}/v$. It can be verified by direct calculations that the function $T_{nl}(v)$ reduces for small v to the corresponding quasistatic expression.⁹

From Eq. (5.14) we can conclude that P_{nl} as a function of n has only one maximum. By direct (but relatively long) calculations we found that the position of selective population maximum $n = n_{\text{max}}$ is determined by

$$n_{\text{max}} \approx \frac{Z}{v} \mathcal{F}(v), \quad (5.15)$$

where $\mathcal{F}(v)$ is a relatively complicate function of v satisfying (at intermediate velocities) simple condition $\mathcal{F}(v)/v \approx 1$. Thus, Eq. (5.15) correlates generally with the experimentally observed trends ($n_{\text{max}} \approx Z$), mentioned in the Introduction. Some specific and intriguing experimental facts about position of the population maxima will be discussed in Sec. V C.

It is worth noting that the first factor Z/v in the Eq. (5.15) represents just the value of $n'_{\text{max}} = Z/v$, calculated by using the simple classical electron pickup model¹⁷ (developed before and outside of discussion of the selective Rydberg levels population). Obviously, this circumstance indicates that the formed Rydberg ions possess some properties of classical objects. Nevertheless, from the expression (5.15) we recognize that only an interplay of classical ($n'_{\text{max}} = Z/v$) and quantum properties [$\mathcal{F}(v) \neq 1$] leads to the more consistent understanding of the selective population of Rydberg states at intermediate velocities.

C. Comparison with experiments

Our final formula for $P_{nl} = P_{nl}(v, Z)$ [Eq. (5.14)] will be compared with experimental data,¹⁻⁸ mentioned in the Introduction. Since our dynamic model holds for point-like ionic cores (see the beginning of Sec. II), it is applicable only to the beam-foil experiments in which hydrogen-like ions (S VI, Cl VII, and Ar VIII) are used.

The population probability $P_{nl} = P_{nl}(v, Z)$ is a complicated function, not only of the quantum numbers n and l , but also of ionic velocity v and the charge Z . For the sake of clarity, among many graphical presentation of $P_{nl}(v, Z)$ we shall prefer mainly those which could be compared with available experimental findings. The experimental studies¹⁻⁸ report only relative population probabilities of Rydberg states, so that some appropriate normalization of the experimental curves to the theoretical predictions will be necessary. We note that the overall uncertainty in the experimentally measured relative level population probabilities is around 20% (see, e.g., Ref. 8).

The n dependence of P_{nl} for ions of sulfur (S VI) and chlorine (Cl VII) is illustrated in Fig. 3(a). We take the case $l = 1$; the values of intermediate ionic velocities v are indicated in the presented figure. The points predicted by our formula (5.14) are connected by solid lines, whereas symbols represent experimental data.⁸ Experimental curves are normalized to the theoretical ones at the population maxima. Curves for $l = 0$ and 2 of S VI and Cl VII ions (with maxima at $n \approx Z$) are similar.

The n dependence of P_{nl} for the argon ion Ar VIII requires more careful analysis. For $l=0$ the shape of the theoretically predicted population curve is similar to those presented in Fig. 3(a): the maximum of the population is at $n \approx 9 \approx Z$, which correlates with experimental data (Ref. 2, Fig. 1). An intriguing situation arises for $l=1$; see Fig. 3(b). In this case, our theoretical curve has expected an "ordinary" shape (with a maximum at $n \approx 8$) whereas the experimental curve² exhibits a dominant maximum at $n=11$. This argon "anomaly" is also found for $l=2$, see Ref. 2, with an almost identical maximum at $n \approx 11$.

The character of the anomalous behavior of Ar VIII will be more transparent if we realize that the experimentally observed shape of the Ar VIII curve can be viewed as a superposition of an "ordinary" curve [dotted curve, Fig. 3(b)] and a dominant peak placed at $n=11$ [dashed curve, Fig. 3(b)]. Obviously, our theoretically

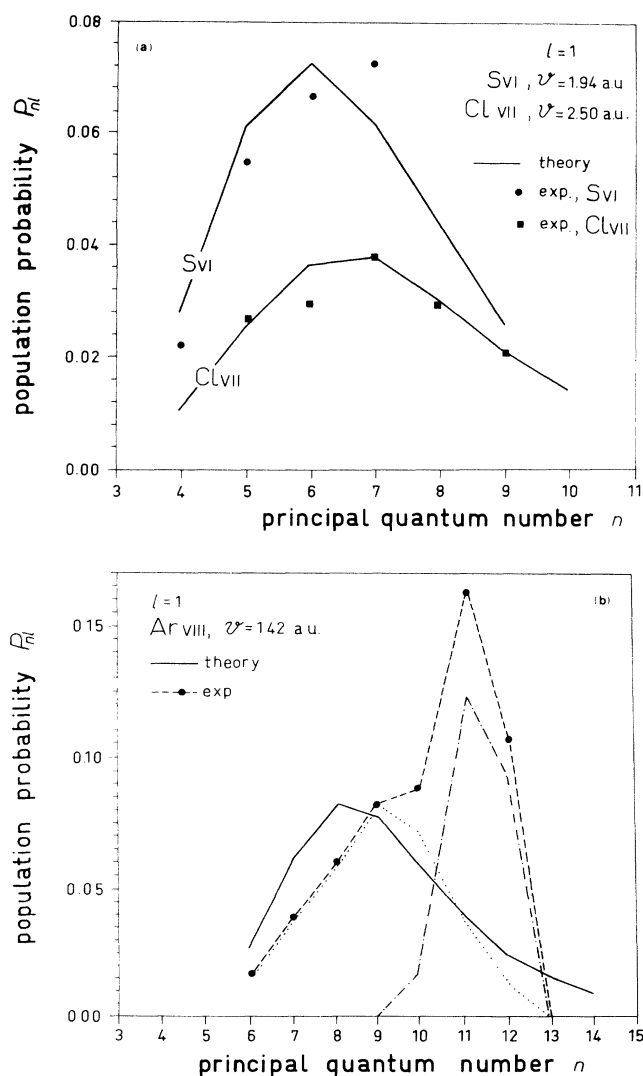


FIG. 3. The n dependence of the population probability P_{nl} for hydrogenlike ions: (a) S VI and Cl VII, (b) Ar VIII. In order to point out the argon "anomaly" the experimentally observed probability distribution (dashed) is decomposed into dotted and the resonancelike curves.

predicted curve [solid line, Fig. 3(b)] is in reasonable agreement with the "modified" experimental (dotted) curve, whose maximum is positioned at $n=9$, i.e., at $n \approx Z=8$. Therefore, the anomaly appears when Z , n , and l , as well as P_{nl} , simultaneously exceed some "critical" values.

From the point of view of the Rydberg state population model presented here, the argon anomaly is not a quite unexpected problem. There are at least two possible reasons why the resonancelike peak at $n=11$ is not contained in our formula for P_{nl} . First, in developing the multichannel formalism (Secs. V A and V B) we restricted ourselves to the case of sufficiently small values of P_{nl} . Second, our wave functions have been calculated for relatively deep underbarrier electron transitions. It is quite possible that only one (or even both) of these assumptions break down in the case of Ar VIII, causing the anomaly. In our concluding remarks (Sec. VI) we shall comment briefly on some possible ways of resolving the problem.

In our Fig. 4 the l dependence of P_{nl} , given by Eq. (5.14), is compared with experiments⁸ (for S VI, Cl VII, and Ar VIII). Corresponding values of n and v are indicated in the figure. We conclude that the agreement of theoretical predictions (solid lines) and experimental results (symbols) is good (in the range of validity of our low-angular-momentum theory, for $l=0, 1$, and 2). In the case of low l , almost identical theoretical curves are obtained for other values of n , as well as for other relevant values of v in the intermediate velocity region. Let us note that, for large l , our theoretical curves decrease with increasing l , so that a detailed comparison with more complicated shapes of experimental curves (see our final comment in Sec. VI) is not sufficiently informative.

The velocity dependence of $P_{nl}=P_{nl}(v, Z)$ for Cl VII and $l=1$ and 2 is presented in Figs. 5(a) and 5(b), respectively. (The theoretical curves for S VI and Ar VIII are similar to the presented ones.) The only available experimental data⁴ for $l=1$ and 2 (indicated by symbols in our

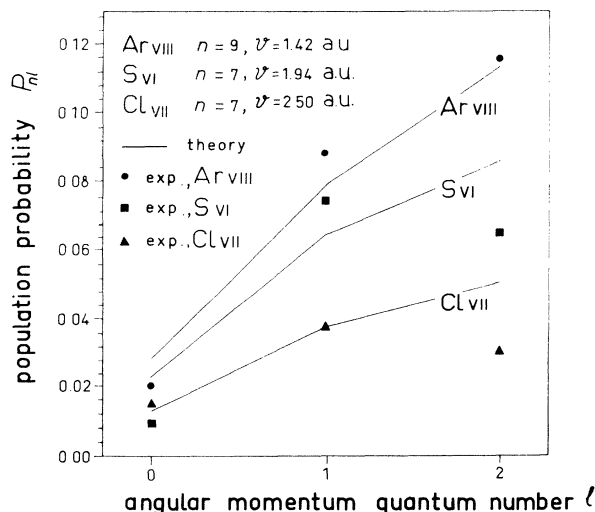


FIG. 4. The l dependence of the population probability P_{nl} for S VI, Cl VII, and Ar VIII in the low-angular-momentum region.

figures) agree satisfactorily with theoretical predictions (solid lines). From the presented figures we see that for $n \approx Z$ the v dependence of $P_{nl}(v, Z)$ has its maximum in just the intermediate velocity region. Such a prediction cannot be deduced from the quasistatic model,⁹ where $P_{nl}(v, Z)$ represents a monotonically decreasing function of v for all Rydberg states and ionic velocities.

Obviously, the presented predictions of the population probability $P_{nl} = P_{nl}(v, Z)$ as a function of n , l , and v (for different ionic charges Z) call for further more systematical and refined experimental studies. Especially, new experimental facts about the v dependence of the population probability P_{nl} could be very useful for deeper understanding of the quantum dynamics of the considered process in the intermediate velocity region.

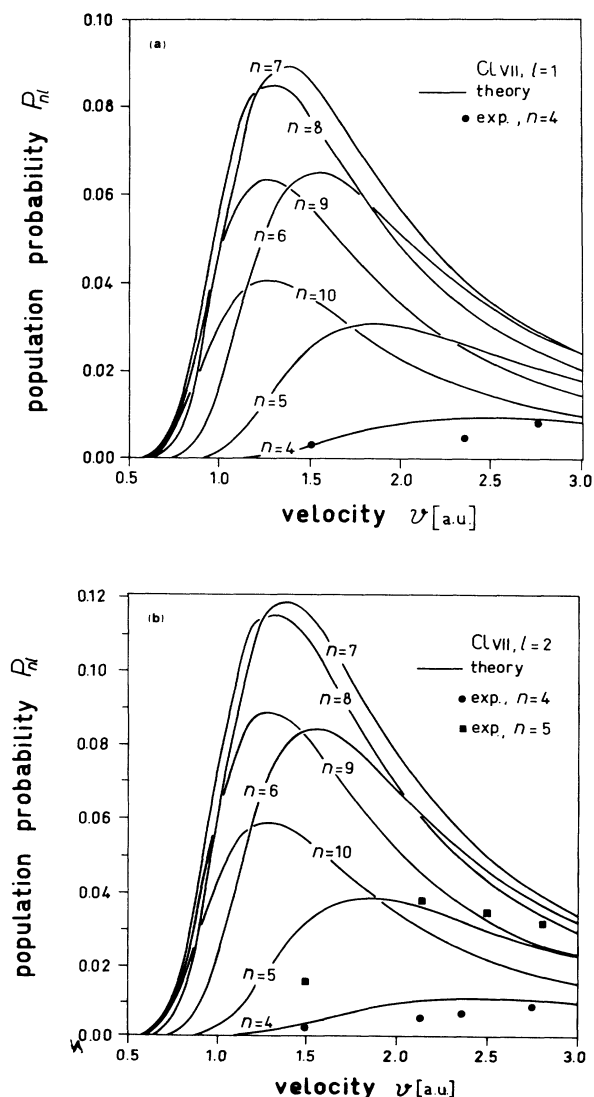


FIG. 5. The v dependence of the population probability P_{nl} for the states: (a) $l=1$ of Cl VII, (b) $l=2$ of Cl VII. Note a nonmonotonic character of all curves, with remarkable maxima just in the intermediate velocity region.

VI. CONCLUDING REMARKS

The analysis performed in this paper leads us to the conclusion that the mechanism of the electron pickup from the foil valence band can be used as a starting point for sufficiently good understanding of experimental data. However, the simple quasiclassical picture¹⁷ of this process, as well as the quasistatic quantum arguments⁹ are not sufficiently informative. Our calculations indicate that only some more elaborate quantum-mechanical treatment of the electron pickup mechanism can elucidate the problem. It was necessary to take into account, as we have seen, both the dynamic character of the process and the main features of the ionic Rydberg states being formed.

Few additional concluding remarks may be relevant for further theoretical work on the proposed electron pickup model in the case of selective Rydberg level population.

First, in the presented model the ionic core has been considered as a pointlike charged particle. As we pointed out, such a structureless particle can be used to describe hydrogenlike ions (e.g., S VI, Cl VII, and Ar VIII) but not the heliumlike species (e.g., Kr VIII and Xe VIII, investigated experimentally in Ref. 3). In the last case, it is reasonable to expect that the screening effect of ionic core electrons can be relevant. In other words, the concepts of the effective projectile charge Z_{eff} and quantum defect δ_{nl} would play some role, especially for low-angular-momentum cases (when Rydberg orbits with high eccentricities partly cross the ionic core; e.g., Ref. 18, Chap. 4.)

Second, the wave functions Ψ_A^{nl} and Ψ_M^{nl} (Secs. III A and III B) used in this paper are basically worked out to describe relatively deep under-barrier electron tunneling. However, it is evident [see, e.g., Fig. 1(b)] that the tunneling near the top of the potential barrier contributes too, especially for sufficiently high n . Let us note that the importance of these electron transitions has been stressed in the context of the Stark ionization (e.g., Ref. 18, Chap. 2). We expect that analogous calculations can also be incorporated into our molecular model.

Third, in this paper the problem of argon anomaly was not discussed in more detail: we mentioned only (Sec. V C) that it can be addressed to the approximations used in developing the multichannel formalism, as well as in evaluation of wave functions. Our preliminary investigations indicate that contribution of the electron transitions near the top of the potential barrier can be relevant. Namely, by using the etalon-equation method (see, e.g., Ref. 18, Chap. 2) for solving quasiradial equation (in the approximation of close turning points) we found a relatively good correlation with an experimentally observed trend of the Ar VIII curve for $n=11, 12,$ and 13 . At present, further elaboration of the presented multichannel formalism seems to be fairly difficult. Even in the approximation of small transition probabilities it is not quite simple to obtain a more precise formula for P_{nl} . We expect that the simple statistical arguments of Sec. V B could be generalized by means of standard models of random processes.^{19,20}

Finally, the available experimental studies¹⁻⁸ report that in the region of high l a decrease combined with a

“saturation” or even with an increase of P_{nl} with increasing l exists. In addition, it was observed⁴ that the maximum of $P_{nl} = P_{nl}(v)$ shifts towards higher ionic velocities when the quantum number n increases. It was suggested²¹ that some additional mechanism (different from the discussed direct pickup from the valence band) could be relevant for the high- l case. In the cited paper,²¹ qualitative description of two such mechanisms, based on the Fano transitions and a capture of secondary electrons, is given.

From the standpoint of the presented molecular model, we do not expect that the additional mechanisms compete in a high degree to the one-electron pickup process. Namely, the mentioned features of the population of high- l Rydberg states could be directly related with the importance of the region, complementary to the narrow cylinder around the z axis (relevant for $l=0,1,2$). At present, we do not have insight in the distribution of the electron-density flux through the S_F plane in this region. We expect that the “bifurcation” methodology,¹⁰ developed for $Z=1$, could be generalized to the case of multiply charged projectiles and that corresponding theory will give correct l behavior.

APPENDIX: CALCULATIONS OF THE DISTORTION FACTORS s_A AND f_A

Inserting Eqs. (3.2a) and (3.2b) into Eq. (3.1) and omitting small terms $\nabla^2 s_A$ and $(\nabla s_A)^2$ we obtain

$$\frac{\nabla \Phi_{A,\gamma_{A0}}}{\Phi_{A,\gamma_{A0}}} \nabla s_A = -(U_M + U_{AM}) + \frac{2Z-1}{4R}. \quad (\text{A1})$$

For large R , the S_F plane will be far from the ionic core, so that the asymptotic form $\Phi_{A,\gamma_{A0}} \sim e^{-\gamma_{A0} r_A}$ for $\Phi_{A,\gamma_{A0}}$ on that plane can be used. Thus

$$\frac{\nabla \Phi_{A,\gamma_{A0}}}{\Phi_{A,\gamma_{A0}}} \approx -\gamma_{A0} \vec{e}_{r_A}, \quad (\text{A2})$$

where \vec{e}_{r_A} is the unit vector of the vector \vec{r}_A .

From (A1) and (A2) we get a simple differential equation for s_A whose general solution is

$$f_A = s_A - S_A = -\frac{2Z-1}{4\gamma_{A0}} \frac{a}{R} + \frac{1}{4} \left[\frac{1}{\gamma_{A0}} - \frac{1}{\gamma_{A0} + iv} \right] \ln \left[1 - \frac{a}{R} \right] - Z \left[\frac{1}{\gamma_{A0}} - \frac{1}{\gamma_{A0} + 2iv} \right] \ln \left[1 - \frac{a}{2R} \right] + (s_{A0} - S_{A0}). \quad (\text{A9})$$

Recalling the boundary condition (3.4) for f_A at $t \rightarrow \infty$ and having in mind Eq. (2.15c) we obtain

$$s_{A0} - S_{A0} = 0, \quad (\text{A10})$$

i.e., the unknown constants cancel. Thus, the final expression for f_A is given by Eq. (3.7).

The remaining unknown constant s_{A0} , Eq. (3.6), can be calculated by using the form of $\Psi_A^{nl}(\vec{r}_A, t)$ in the adiabatic

$$s_A = -\frac{2Z-1}{4\gamma_{A0}R} r_A + \frac{1}{\gamma_{A0}} \int_0^{r_A} (U_M + U_{AM}) dr_A + s_{A0}. \quad (\text{A3})$$

The explicit form of the obtained solution in the central part of the S_F plane ($r_A \approx a$) is given by (3.6).

In order to calculate the space-time distortion factor f_A we write the $\Psi_A^{nl}(\vec{r}_A, t)$ function, Eq. (3.3), in the following form:

$$\Psi_A^{nl} = \Phi_{A,\gamma_{A0}} e^{-S_A(\vec{r},t) + (i/2)\gamma_{A0}^2 t}, \quad (\text{A4})$$

where

$$S_A(\vec{r}, t) = s_A - f_A. \quad (\text{A5})$$

Inserting the Eq. (A4) into the Schrödinger equation

$$i \frac{\partial \Psi_A^{nl}}{\partial t} = H \Psi_A^{nl},$$

neglecting the small terms $\nabla^2 S_A$ and $(\nabla S_A)^2$, and using relation (A2), we obtain

$$i \frac{\partial S_A}{\partial t} - \gamma_{A0} \frac{\partial S_A}{\partial r_A} = -(U_M + U_{AM}). \quad (\text{A6})$$

This partial differential equation can be solved by using complex variables^{10,11}

$$\xi_A = -\frac{1}{2} \left[\frac{1}{\gamma_{A0}} r_A + it \right], \quad \eta_A = \frac{1}{2} \left[\frac{1}{\gamma_{A0}} r_A - it \right]. \quad (\text{A7})$$

In the central part of the S_F plane we obtain

$$S_A = \frac{1}{4(\gamma_{A0} + iv)} \ln \left[1 - \frac{a}{R} \right] - \frac{Z}{\gamma_{A0} + 2iv} \ln \left[1 - \frac{a}{2R} \right] + S_{A0}, \quad (\text{A8})$$

where S_{A0} is a free constant of integration.

Now, using (A8), (A5), and (A3) we get

limit ($v \approx 0, R \approx \text{const}$). In this case, the function $\Psi_A^{nl}(\vec{r}_A, t)$ can be roughly taken to be stationary state of the following from:

$$\Psi_A^{nl}(\vec{r}_A, t) \rightarrow \Phi_{A,\gamma_A}(\vec{r}_A, R) e^{-iE_A(R)t}, \quad (\text{A11})$$

where Φ_{A,γ_A} is defined by

$$(-\frac{1}{2}\nabla^2 + U_A)\Phi_{A,\gamma_A}(\vec{r}_A, R) = E_A(R)\Phi_{A,\gamma_A}(\vec{r}_A, R), \quad (\text{A12})$$

whereas $E_A(R)$ is given by Eq. (3.2b). In other words, the hydrogenlike function Φ_{A,γ_A} corresponds to the atomic energy level $-\gamma_{A0}^2/2$ shifted upwards by the image force interaction

$$U_A + U_{AM} \approx \frac{2Z-1}{4R}.$$

On the S_F plane and for large R we have

$$\Phi_{A,\gamma_A}(\vec{r}_A, R) \approx \Phi_{A,\gamma_{A0}}(\vec{r}_A, R) \exp\left[\frac{2Z-1}{4\gamma_{A0}} \frac{r_A}{R}\right], \quad (\text{A13})$$

where $\Phi_{A,\gamma_{A0}}$ is defined by Eq. (2.4).

Therefore, in order to find the unknown constant s_{A0} we ought to calculate Ψ_A^{nl} [defined by (3.3), (3.2a), and (3.6)] for $v \approx 0$ and $R \approx \text{const}$, and compare the obtained solution with the adiabatic form given by Eq. (A11). This procedure gives

$$s_{A0} = -\frac{2Z-1}{2\gamma_{A0}} \frac{a}{R} + \left[\frac{2Z-1}{4\gamma_{A0}} \frac{a}{R} - \frac{1}{4\gamma_{A0}} \ln\left[1 - \frac{a}{R}\right] + \frac{Z}{\gamma_{A0}} \ln\left[1 - \frac{a}{2R}\right] \right] + i \frac{2Z-1}{4v}. \quad (\text{A14})$$

The second term [] in the real part of Eq. (A14) can be neglected in comparison with the first one (this may be verified by direct numerical calculation taking, for example, the characteristic values of relevant parameters Z , $\gamma_{A0} = Z/n \approx 1$, and $a/R \approx \frac{1}{2}$). In this way, we obtain the expression (3.8) as a sufficiently good approximation of (A14).

Let us note, that although the Φ_{AM} function [Eq. (3.2a)] becomes the atomic function $\Phi_{A,\gamma_{A0}}$ in the vicinity of the ionic core, this circumstance cannot be used in the calculation of s_{A0} . Indeed, the obtained expressions (A3) and (A8) are valid exclusively on the S_F plane, i.e., they cannot be extrapolated in the vicinity of the ionic core. This fact motivated the use of the adiabatic limit condition (A11).

¹B. Andresen, B. Denne, J. O. Ekberg, L. Engström, S. Huldt, I. Martinson, and E. Veje, *Phys. Rev. A* **23**, 479 (1981).

²S. Bashkin, H. Oona, and E. Veje, *Phys. Rev. A* **25**, 417 (1982).

³R. Hallin, J. A. Leavitt, A. Lindgard, P. W. Rathmann, H. Vach, and E. Veje, *Nucl. Instrum. Methods* **202**, 41 (1982).

⁴C. Jupén, B. Denne, J. O. Ekberg, L. Engström, U. Litzén, I. Martinson, W. Tai-Meng, A. Trigueiros, and E. Veje, *Phys. Rev. A* **26**, 2468 (1982).

⁵L. Engström, *Phys. Scr.* **28**, 68 (1983).

⁶H. Winter, R. Zimny, A. Schirmacher, B. Becker, H. J. Andrä, and R. Fröhling, *Z. Phys. A* **311**, 267 (1983).

⁷E. Veje, *Nucl. Instrum. Methods* **B 9**, 586 (1985).

⁸E. Veje and H. Winter, *Z. Phys. D* **10**, 457 (1988).

⁹R. K. Janev and S. B. Vojvodić, *J. Phys. B* **13**, 2481 (1980); R. K. Janev, *ibid.* **7**, 1506 (1974).

¹⁰N. N. Nedeljković, Lj. D. Nedeljković, R. K. Janev, and Z. L. Mišković, *Nucl. Instrum. Methods* **B 58**, 519 (1991).

¹¹Yu. N. Demkov and V. N. Ostrovskii, *Zh. Eksp. Teor. Fiz.* **69**, 1582 (1975) [*Sov. Phys. JETP* **42**, 806 (1976)].

¹²P. Appel, *Nucl. Instrum. Methods* **B 58**, 519 (1991).

¹³M. Abramovitz and I. Stegun, *Handbook of Mathematical Functions* (Dover, New York, 1972).

¹⁴H. B. Michaelson, *J. Appl. Phys.* **48**, 4729 (1977).

¹⁵K. Blum, *Density Matrix: Theory and Applications* (Plenum, New York, 1981), Chaps. 5.1 and 7.3.

¹⁶A. Messiah, *Quantum Mechanics* (North-Holland, Amsterdam, 1970), Vol. I, p. 110.

¹⁷D. G. Ellis, *J. Phys. (Paris)* **40**, Cl-152 (1979).

¹⁸*Rydberg States of Atoms and Molecules*, edited by R. F. Stebbings and F. B. Dunning (Cambridge University Press, New York, 1983).

¹⁹H. Haken, *Synergetics* (Springer-Verlag, Berlin, 1978), Chaps. 4 and 3.

²⁰G. M. Zaslavsky, R. Z. Sagdeev, D. A. Usikov, and A. A. Chernikov, *Weak Chaos and Quasi-Regular Patterns* (Nauka, Moscow, 1991), Chap. 3 (in Russian).

²¹S. Bashkin, E. Träbert, P. H. Heckmann, and H. V. Buttlar, *Phys. Scr.* **28**, 193 (1983).